

Amplifier Linearization by Using the Generalized Baseband Signal Injection Method

LEUNG Chi-Shuen

A Thesis Submitted in Partial Fulfillment

of the Requirements for the degree of

Master of Philosophy

in

Electronic Engineering

©The Chinese University of Hong Kong

June 2002

The Chinese University of Hong Kong holds the copyright of this thesis. Any person(s) intending to use a part or whole of the materials in the thesis in a proposed publication must seek copyright release from the Dean of the Graduate School.



Abstract

In recent years, there has been a phenomenal growth in wireless communications. Because of the demand on high data rate applications and the request of efficient utilization of the increasingly crowded spectrum, spectral efficient linear modulation schemes have to be employed which require ultra linear amplifier for amplification. In the past years, various linearization methods have been addressed that offer different degree of performance at the expense of circuit complexity. Unfortunately, most of these methods require costly and bulky RF circuitry that is not suitable for mobile terminals.

In this thesis, the new concept of generalized baseband signal injection is introduced. The applications of the proposed method to the linearization of various configurations of amplifying systems are described. A general and rigorous mathematical formulation of the new approach is also presented. Unlike many conventional approaches, no complex RF circuitry is required other than simple baseband amplifiers.

For verification purposes, two amplifying systems operating at approximately 2GHz are constructed and characterized. Good agreements between the theoretical and experimental results are observed based on the two-tone and vector signal test measurements.

摘要

近年來，由於無線通訊的蓬勃發展，高頻譜效率的調變方案將會被採用以解決大容量數據傳輸的需求和有效地使用日益擁擠的頻譜。高頻譜效率的調變方案要求高線性的訊號放大器，而在過往的文獻中也記載了各種的方法，以不同複雜程度的電路來實現線性放大的要求。不幸的是，這大多數現有的建議都需要昂貴且體積龐大的射頻電路，因此並不適用於小巧的無線終端機。

本論文提出廣義基頻訊號注入的新概念，並在不同配置的放大系統中的實際應用。本文對所提出之新方法也作了全面和嚴謹的數學推導。和過往許多方法不同的是，除了基頻放大器外，此方法並不需要複雜的射頻電路。

爲了驗證所提出之新概念，我們設計並製造了兩組約爲2千兆赫的放大系統。在使用雙頻訊號和向量訊號作測試的情況下，發現理論與實驗結果都非常吻合。

Acknowledgement

I would like to express my gratitude to my supervisor, Prof. K. K. M. Cheng, for his guidance and understanding. His insight and persistence in research have enlightened me so much.

I would like to express my sincere thanks to Dr. C. W. Fan for his suggestions and helpful discussions in my research. Thanks are also extended to my colleagues in Microwave Laboratory for their help. Special thanks to colleagues, Mr. Chan Shek Hang and Mr. Tsang Wai Mong, for sharing with me their findings and joy.

I would like to acknowledge the support of my parents. I am gratefully indebted to my beloved mother.

Table of Content

Chapter 1	Introduction	1
Chapter 2	Review of Linearization Techniques	4
2.1	Feedforward	5
2.2	Feedback	7
2.3	Predistortion	10
Chapter 3	The Volterra Series Method for Nonlinear Analysis	12
3.1	Volterra Series Method	13
3.2	Nonlinear Transfer Function	14
3.3	Weakly Nonlinear Approximation	18
3.4	Nonlinear Modeling	19
3.5	Determination of Nonlinear Transfer Function	22
Chapter 4	Manifestation of Nonlinear Behavior	25
4.1	Two-Tone Volterra Series Analysis	25
4.2	Harmonic Distortion	28
4.3	AM/AM and AM/PM	29
4.4	Intermodulation Distortion	31
Chapter 5	The Generalized Baseband Signal Injection Method	33
5.1	Generalized Baseband Signal Injection Method (GM)	34
5.2	Application of GM to Predistorter-Amplifier Linearization	38
5.2.1	Case 1: Standalone Amplifier without Injection	40
5.2.2	Case 2: Injection to Amplifier Only	41
5.2.3	Case 3: Injection to Diode Predistorter Only	41
5.2.4	Case 4: Injection to Both Diode Predistorter and Amplifier	42
5.3	Application of GM to Multi-Stage Amplifier Linearization	43
5.3.1	Case 1: Amplifying System with No Signal Injection	46
5.3.2	Case 2: Amplifying System with Single Injection Point	47
5.3.3	Case 3: Amplifying System with Two Injection Points	48
Chapter 6	Experimental Setup and Measurements	50
6.1	Experimental Setup	51
6.1.1	Diode Predistorter	51
6.1.2	Small Signal Amplifier	54
6.1.3	Medium Power Amplifier	58
6.1.4	Baseband Signal Generation Circuit	61
6.1.5	Baseband Amplifiers	63
6.2	Linearization of Amplifier with Predistortion Circuitry	65

6.2.1	Two-Tone Test	65
6.2.2	Vector Signal Test	68
6.2.3	Dynamic Range Evaluation	70
6.3	Linearization of Multi-Stage Amplifying System	71
6.3.1	Determination of Transfer and Gain Coefficients	71
6.3.2	Two-Tone Test	74
6.3.3	Vector Signal Test	77
6.3.4	Dynamic Range Evaluation	79
Chapter 7	Conclusion and Future Work	80
	References	82
	Author's Publications	90

Chapter 1 Introduction

Power amplifier is one of the crucial functional blocks in wireless communication systems. The modulated RF signal is amplified to reach the required power level before transmission. In traditional communication systems, constant envelope modulation formats, such as FM used in AMPS system and GMSK employed in GSM system, are adopted. For these modulation schemes, either frequency or phase of the carrier is utilized for carrying information and therefore linearity of the power amplifier is not of main concern. As a result, highly efficient, nonlinear amplifiers (eg, class B and C) are widely used for power saving, with the drawback of poor spectral efficiency. Spectral efficiency of constant envelope modulation schemes is limited to 1bit/s/Hz.

In recent years, there has been a rapid growth in the wireless market for high speed and reliable data transmission that requires the use of spectral efficient linear modulation schemes including QPSK, QAM and OFDM. Both phase and amplitude of RF carrier are modulated for carrying information. Hence, the modulated RF carrier possess time varying envelope waveform. When this signal is injected into nonlinear amplifier, severe distortions are generated. The in-band distortion causes impairment in transmitted signal while the out-of-band emission causes undesired

interference to adjacent channels. Moreover, even in traditional communication systems where constant envelope modulation formats are adopted, it is more convenient and cost effective to transmit multi-carrier signals through a single amplifier rather than using numerous amplifiers with power combiners and splitters. All in all, linear amplifiers are desirable in modern wireless communication systems.

In order to satisfy the low distortion requirement, the traditional way is to operate the amplifiers several dB backoff from saturation, with the drawback of low power efficiency. In the past years, various linearization methods [1] have been proposed. They offer different degree of linearity improvement at the expense of cost, size and complexity. Unfortunately, most of these methods require costly and bulky RF circuitries that limit them to basestation application only. For battery powered mobile handsets, cost and size are important factors along with high linearity requirement. Compact and effective linearization schemes are therefore in need.

In recent years, several linearization methods based on second-order signal injection have also been reported [2-5]. IMD suppression has been achieved by exploiting the second-order nonlinearity and second-order signal at either difference frequency and second harmonic. From a practical point of view, difference frequency approach is simpler to implement but can only give limited IMD improvement. On the other hand, the second harmonic injection technique offers substantial IMD

improvement with the drawback of requiring precise RF gain and phase adjustment. Recently, Fan and Cheng introduce the simultaneous harmonic and baseband injection [6] and the constraint of precise phase adjustment is relaxed.

In this research, a new linearization concept is introduced, namely the generalized baseband signal injection method. The proposed method has the advantages over conventional techniques in terms of compact size, low circuit complexity, unconditionally stable, has little effect on amplifier gain, power efficient and amendable to integrated circuit design.

This thesis is divided into 7 chapters. Chapter 2 is a review on some popular linearization techniques. Chapter 3 introduces the Volterra series method for analyzing nonlinear systems. Methods of modeling nonlinear elements are also addressed. In Chapter 4, different kinds of distortion are identified by two-tone Volterra series analysis. Chapter 5 details the generalized baseband signal injection method and its application to the linearization of microwave amplifiers. Operating conditions for optimum IMD suppression are also derived. Experimental circuit construction and measurements are described in Chapter 6. Finally, Chapter 7 concludes this thesis with recommendations for future developments.

Chapter 2 Review of Linearization Techniques

A wide range of linearization techniques have been proposed over the years. Broadly speaking, linearization techniques can be classified into three main streams: feedforward [7-13], feedback [14-17] and predistortion [18-23]. There are also combinations of them [24-26]. In this chapter, the basics of the above three techniques are reviewed.

Besides these methods, a variety of other approaches have also been reported such as envelope elimination and restoration [27, 28], linear amplification using nonlinear components [29, 30], combined analogue-locked loop universal modulator method [31, 32] and linear amplification using sampling technique [33]. Digital signal processing techniques are used in these methods for separating the envelope and phase information of the modulated RF signal. Thus power efficient and nonlinear amplifiers can be employed for the synthesis of linear output. Theoretically, the above techniques can approach 100% power efficiency but their perceived complexity hinder them from practical use. Their principles are not given here and readers may refer to the corresponding references for details.

2.1 Feedforward

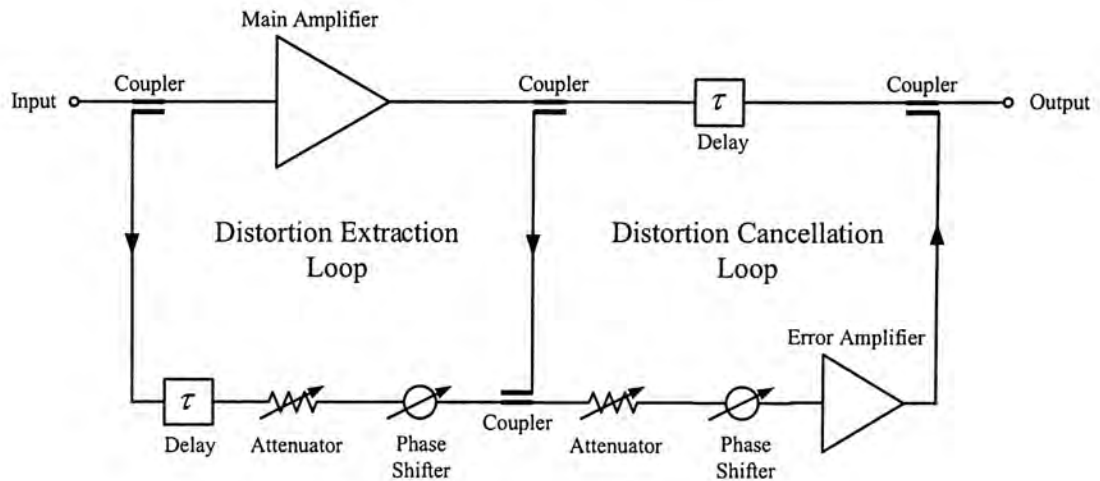


Fig. 2.1 Feedforward system

Fig. 3.2 shows the basic configuration of a feedforward system [7] which consists of two signal loops: the distortion extraction loop and the distortion cancellation loop. In the distortion extraction loop, the distorted output signal of the main amplifier is sampled and then subtracted from the delayed version of the input signal. By the careful adjustment of the magnitude and phase of signal in the lower path of the distortion extraction loop, the main tones can be suppressed leaving the distortion components. In the distortion cancellation loop, the extracted distortion signal is phase shifted, amplified and added onto the output of the system. Again, by the careful adjustment of magnitude and phase shift of the extracted distortion signal, distortion at the output of the system can be cancelled out and leaving the linear amplified signal only.

Feedforward linearization offers superior linearity performance but requires

complex and bulky circuitry:

1. The error amplifier has to be ultra linear, any distortion generated by it will appear at the output of the system. Hence, low efficiency linear amplifier must be adopted.
2. Usually, lossy coaxial cable which is located after the main amplifier is used for compensating delay between the upper and lower path of the distortion cancellation loop. Delay introduced by the error amplifier should be as little as possible for minimal insertion loss caused by coaxial cables [8].
3. Coupling ratio of the output coupler has to be carefully selected for smaller power loss while keeping the power handling capability of the error amplifier at a reasonable level [9].
4. Both loops in the feedforward system are highly sensitive to phase mismatch and amplitude mismatch. In order to achieve sufficiently low of IMD level against shift of parameters such as temperature, adaptive adjustments of the attenuators and phase shifters are necessary. Examples of analog and digital adaptive controlled feedforward system can be found in [10-13].

Generally speaking, feedforward linearization is only suitable for implementation in basestation and is too complex and expensive for portable devices.

2.2 Feedback

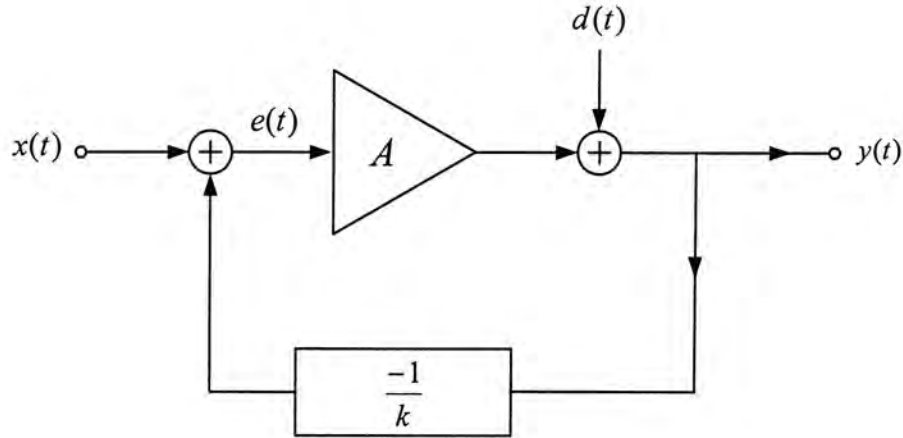


Fig. 2.2 Feedback system

Feedback is probably the simplest technique for reducing amplifier distortion and is widely used in low frequency circuit design. A generalized feedback system is shown in Fig. 2.2. Input and output to the amplifier is represented by $x(t)$ and $y(t)$, respectively. Distortion generated by the amplifier is modeled by $d(t)$ and k is a constant account for the sampling of output signal. The relation between input and output of the system can be formulated as:

$$y(t) = Ax(t) + d(t) \quad (2.1)$$

The error signal is given by:

$$e(t) = x(t) - \frac{y(t)}{k} \quad (2.2)$$

Substituting (2.2) into (2.1) and assuming $A \gg k$, we have:

$$y(t) \approx k \left[x(t) + \frac{d(t)}{A} \right] \quad (2.3)$$

Equation (2.3) indicates gain of the amplifier drop with a factor of $\frac{k}{A}$ and distortion

is suppressed with a factor of $\frac{k}{A}$, the sacrifice in gain is exchanged for improvement in distortion. At low frequency, high gain amplifier is easy to design and feedback is usually employed for improving distortion performance. But the situation at microwave frequency is different as gain of RF amplifier is luxurious. Also, in the above derivation, it is assumed that time delays introduced by the amplifier and other circuitry are negligible comparing with the frequency of the input signal. This is certainly not the case for RF circuits. Hence, conventional feedback is seldom used in RF amplifier design.

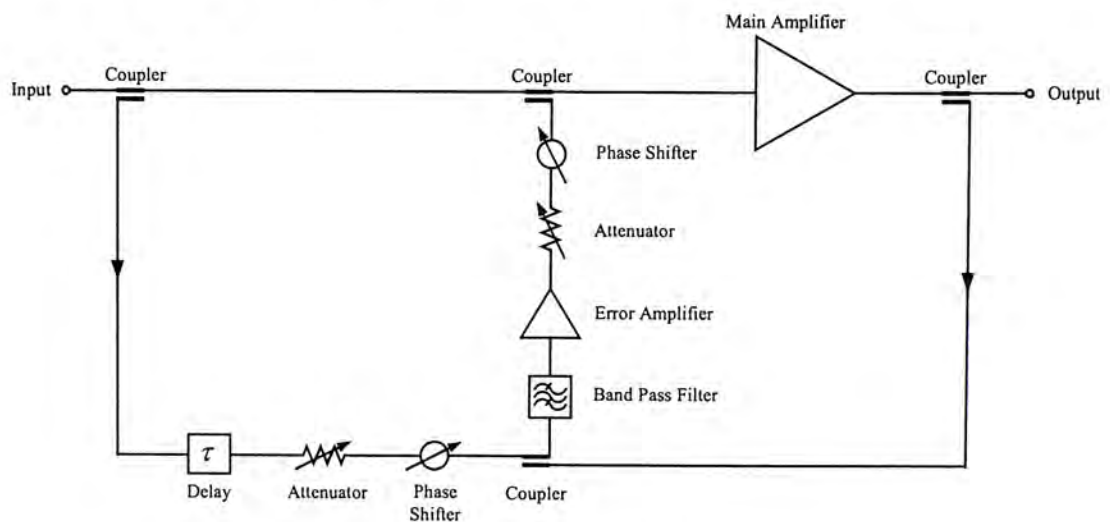


Fig. 2.3 Distortion feedback system

In [14], distortion feedback is proposed and the configuration of distortion feedback system is shown in Fig. 2.3. By means of couplers, a portion of the distorted output is sampled. By subtracting the sampled output signal with the input signal and by the proper adjustment of attenuator and phase shifter, distortion generated by the main amplifier can be extracted. The extracted distortion is then

phase shifted, amplified and injected back to the input of the system. Band-pass filter is used for suppressing any out-of-band signal that may cause instability. Time delay introduced by the main amplifier, the error amplifier, filter and any other components must be considered for ensuring stability. Generally speaking, feedback system is only applicable in narrow band operation. Adaptive control of the attenuators and phase shifters is still required for maintaining proper operation of the system.

Other feedback linearization techniques can be found in literature, such as cartesian feedback [15, 16] and envelope feedback [17]. In these methods, down-converted baseband signal is employed as the feedback signal rather than the RF signal.

2.3 Predistortion

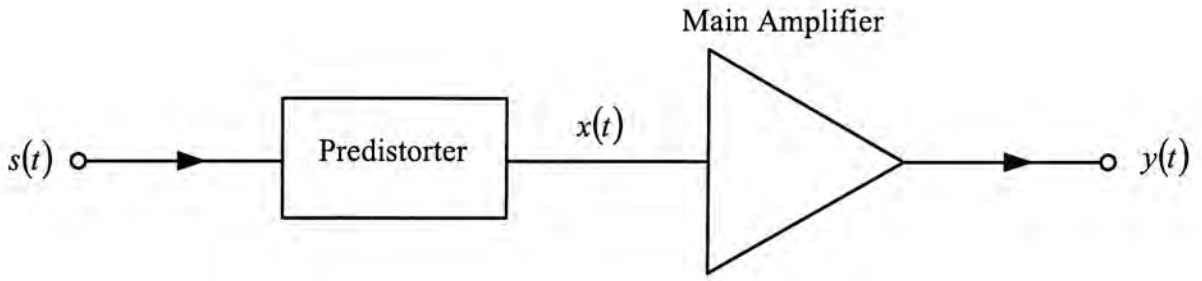


Fig. 2.4 Predistorted system

Predistortion involves the creation of distortion characteristic that is complementary to the amplifier being linearized as shown in Fig. 2.4. For the purpose of illustration, both the predistorter and the amplifier are assumed memoryless, and the transfer characteristic of the predistorter and the amplifier are described by:

$$x(t) = a_1 s(t) + a_2 s^2(t) + a_3 s^3(t) + \dots \quad (2.4)$$

$$y(t) = b_1 x(t) + b_2 x^2(t) + b_3 x^3(t) + \dots \quad (2.5)$$

Combining (2.4) and (2.5), we have:

$$\begin{aligned} y(t) = & a_1 b_1 s(t) + \\ & a_2 b_1 s^2(t) + a_1^2 b_2 s^2(t) + \\ & a_3 b_1 s^3(t) + 2a_1 a_2 b_2 s^3(t) + a_1^3 b_3 s^3(t) + \dots \end{aligned} \quad (2.6)$$

Let A be the gain of the predistorted system, where

$$A = a_1 b_1 \quad (2.7)$$

Neglect all the nonlinear terms with degree higher than three, distortions can be cancelled out by setting:

$$a_2 = \frac{-b_2}{b_1^3} A^2 \quad (2.8)$$

$$a_3 = \frac{2b_2^2 - b_1 b_3}{b_1^5} A^3 \quad (2.9)$$

Usually, the value of a_2 is not of concern as second order distortions generated are one carrier frequency away and can be eliminated by filtering techniques. The predistorter can be implemented by varactor diode [18], Schottky diode [19, 20], FET [21, 22] or even amplifier [23]. They offer different degree of improvement at the expense of circuit complexity. Because of the inherent open loop properties, predistorted system is unconditionally stable and the operational bandwidth is much wider than that of feedback system. Generally speaking, predistorted system is much simpler and more power efficient than feedforward system. On the other hand, predistortion technique can only suppress the specific order of distortion, usually the third-order or at most the fifth-order distortion, over a small range of input power.

Chapter 3 The Volterra Series Method for Nonlinear Analysis

In this chapter, the basic theory of Volterra series is introduced. Comparing to other nonlinear analysis techniques such as Spice and harmonic balance, Volterra series method operate entirely in the frequency domain. As a result, steady state response of the nonlinear system can be obtained directly. Furthermore, the calculation process is non-iterative and no computational intensive fast Fourier transform algorithm is needed. And the most important, Volterra series analysis is capable of expressing nonlinear behaviors explicitly in terms of circuit parameters.

Power series analysis is another widely accepted method for analyzing nonlinear system. Indeed, it does give circuit designer an intuitive sense on the behavior of nonlinear circuits. But power series requires an unrealistic assumption that the system to be analyzed is memoryless [34]: Output of the system at time t depends only on the input at the same instant.

$$v_o(t) = a_0 + a_1 v_i(t) + a_2 v_i^2(t) + a_3 v_i^3(t) + \dots \quad (3.1)$$

where a_n are real-valued, frequency independent coefficients.

Volterra series can be viewed as a generalization of power series with memory effect included, output of nonlinear system at time t depend on not only the input at present but also the past history.

3.1 Volterra Series Method

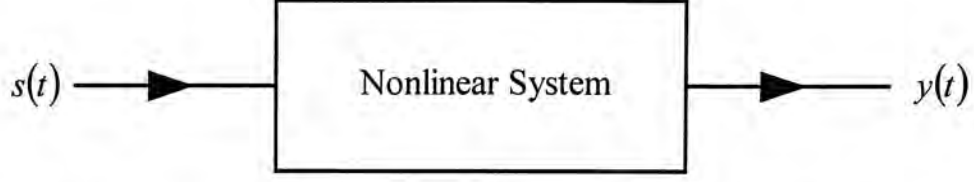


Fig. 3.1 Nonlinear system model for Volterra series analysis

A nonlinear system model used for Volterra series analysis is shown in Fig. 3.1.

The nonlinear system may contain a mix of linear and nonlinear elements with either frequency independent or frequency dependent properties. The excitation and output to the system are represented by $s(t)$ and $y(t)$, respectively. The excitation signal $s(t)$ may contain a number of discrete signal tones at different frequencies:

$$\begin{aligned} s(t) &= v_{s,1} \cos(\omega_1 t) + v_{s,2} \cos(\omega_2 t) + \dots + v_{s,Q} \cos(\omega_Q t) \\ &= \frac{1}{2} \sum_{\substack{q=-Q \\ q \neq 0}}^Q v_{s,q} e^{j\omega_q t} \end{aligned} \quad (3.2)$$

where q is the frequency index. The case $q=0$ is excluded as it represents DC signal.

Consequently, the system output is given by:

$$y(t) = \sum_{n=1}^{\infty} \frac{1}{2^n} \sum_{\substack{q_1=-Q \\ q_1 \neq 0}}^Q \sum_{\substack{q_2=-Q \\ q_2 \neq 0}}^Q \dots \sum_{\substack{q_n=-Q \\ q_n \neq 0}}^Q H_n(\omega_{q_1}, \omega_{q_2}, \dots, \omega_{q_n}) v_{s,q_1} v_{s,q_2} \dots v_{s,q_n} e^{j(\omega_{q_1} + \omega_{q_2} + \dots + \omega_{q_n})t} \quad (3.3)$$

where $H_n(\omega_{q_1}, \omega_{q_2}, \dots, \omega_{q_n})$ is the n -th order nonlinear transfer function. With the nonlinear transfer functions known and by summing the responses from 1 to ∞ , the overall response of the system can be determined. Note that $H_1(\)$ is actually the transfer function of the linearized system.

3.2 Nonlinear Transfer Function

For a linear and time invariant system having excitation $s(t)$. The output $y(t)$ can be expressed by the convolution integral:

$$y(t) = \int_{-\infty}^{\infty} h(\tau) s(t - \tau) d\tau \quad (3.4)$$

where $h(t)$ is the impulse response of the system. For nonlinear system, the linear relation between $y(t)$ and $s(t)$ can no longer be applied.

Volterra showed that any continuous function, $f(x)$, can be represented by the expansion:

$$f(x) = \sum_{n=0}^{\infty} f_n(x) \quad (3.5)$$

where $f_n(x)$ is a regular homogeneous functional such that:

$$f_n(x) = \int_{-\infty}^{\infty} \int_{-\infty}^{\infty} \dots \int_{-\infty}^{\infty} h_n(\xi_1, \xi_2, \dots, \xi_n) x(\xi_1) x(\xi_2) \dots x(\xi_n) d\xi_1 d\xi_2 d\xi_3 \quad (3.6)$$

Norbert Wiener applied the work of Volterra to the analysis of nonlinear systems.

Wiener suggested that the output of a nonlinear system may be represented by a functional series in term of its input [35]:

$$\begin{aligned}
 y(t) = & \int_{-\infty}^{\infty} h_1(\tau) s(t-\tau) d\tau \\
 & + \int_{-\infty}^{\infty} \int_{-\infty}^{\infty} h_2(\tau_1, \tau_2) s(t-\tau_1) s(t-\tau_2) d\tau_1 d\tau_2 \\
 & + \int_{-\infty}^{\infty} \int_{-\infty}^{\infty} \int_{-\infty}^{\infty} h_3(\tau_1, \tau_2, \tau_3) s(t-\tau_1) s(t-\tau_2) s(t-\tau_3) d\tau_1 d\tau_2 d\tau_3 \\
 & + \dots
 \end{aligned} \tag{3.7}$$

Expression (3.7) can be re-expressed as:

$$y(t) = \sum_{n=1}^{\infty} y_n(t) \tag{3.8}$$

where

$$y_n(t) = \int_{-\infty}^{\infty} \int_{-\infty}^{\infty} \dots \int_{-\infty}^{\infty} h_n(\tau_1, \tau_2, \dots, \tau_n) s(t-\tau_1) s(t-\tau_2) \dots s(t-\tau_n) d\tau_1 d\tau_2 \dots d\tau_n \tag{3.9}$$

The function $h_n(\tau_1, \tau_2, \dots, \tau_n)$ is known as the n -th order kernel or the n -th order nonlinear impulse response. Note that the zeroth-order kernel is excluded as it accounts for the response to DC input.

By substituting (3.2) into (3.9), we have:

$$\begin{aligned}
 y_n(t) = & \frac{1}{2^n} \int_{-\infty}^{\infty} \int_{-\infty}^{\infty} \dots \int_{-\infty}^{\infty} h_n(\tau_1, \tau_2, \dots, \tau_n) \sum_{\substack{q_1=-Q \\ q_1 \neq 0}}^Q v_{s,q_1} e^{j\omega_{q_1}(t-\tau_1)} \\
 & \cdot \sum_{\substack{q_2=-Q \\ q_2 \neq 0}}^Q v_{s,q_2} e^{j\omega_{q_2}(t-\tau_2)} \dots \sum_{\substack{q_n=-Q \\ q_n \neq 0}}^Q v_{s,q_n} e^{j\omega_{q_n}(t-\tau_n)} d\tau_1 d\tau_2 \dots d\tau_n
 \end{aligned} \tag{3.10}$$

Rearranging the terms in (3.10), interchanging the order integration and summation gives:

$$\begin{aligned}
 y_n(t) = & \frac{1}{2^n} \sum_{\substack{q_1=-Q \\ q_1 \neq 0}}^Q \sum_{\substack{q_2=-Q \\ q_2 \neq 0}}^Q \dots \sum_{\substack{q_n=-Q \\ q_n \neq 0}}^Q v_{s,q_1} v_{s,q_2} \dots v_{s,q_n} e^{j(\omega_{q_1} + \omega_{q_2} + \dots + \omega_{q_n})t} \\
 & \cdot \int_{-\infty}^{\infty} \int_{-\infty}^{\infty} \dots \int_{-\infty}^{\infty} h_n(\tau_1, \tau_2, \dots, \tau_n) e^{j(\omega_{q_1}\tau_1 + \omega_{q_2}\tau_2 + \dots + \omega_{q_n}\tau_n)} d\tau_1 d\tau_2 \dots d\tau_n
 \end{aligned} \tag{3.11}$$

The multidimensional Fourier transform of the n -th order nonlinear impulse response in (3.11) can now be recognized as:

$$H_n(\omega_{q_1}, \omega_{q_2}, \dots, \omega_{q_n}) = \int_{-\infty}^{\infty} \int_{-\infty}^{\infty} \dots \int_{-\infty}^{\infty} h_n(\tau_1, \tau_2, \dots, \tau_n) e^{-j(\omega_{q_1}\tau_1 + \omega_{q_2}\tau_2 + \dots + \omega_{q_n}\tau_n)} d\tau_1 d\tau_2 \dots d\tau_n \tag{3.12}$$

Conversely, the n -th order nonlinear impulse response can be found from the n -th order nonlinear transfer function via inverse Fourier transform:

$$\begin{aligned}
 h_n(\tau_1, \tau_2, \dots, \tau_n) = & \frac{1}{(2\pi)^n} \int_{-\infty}^{\infty} \int_{-\infty}^{\infty} \dots \int_{-\infty}^{\infty} H_n(\omega_{q_1}, \omega_{q_2}, \dots, \omega_{q_n}) \\
 & \cdot e^{j(\omega_{q_1}\tau_1 + \omega_{q_2}\tau_2 + \dots + \omega_{q_n}\tau_n)} d\omega_{q_1} d\omega_{q_2} \dots d\omega_{q_n}
 \end{aligned} \tag{3.13}$$

Replacing the integrals in (3.11) with the nonlinear transfer function $H_n(\omega_{q_1}, \omega_{q_2}, \dots, \omega_{q_n})$ gives:

$$y_n(t) = \frac{1}{2^n} \sum_{\substack{q_1=-Q \\ q_1 \neq 0}}^Q \sum_{\substack{q_2=-Q \\ q_2 \neq 0}}^Q \dots \sum_{\substack{q_n=-Q \\ q_n \neq 0}}^Q H_n(\omega_{q_1}, \omega_{q_2}, \dots, \omega_{q_n}) v_{s,q_1} v_{s,q_2} \dots v_{s,q_n} e^{j(\omega_{q_1} + \omega_{q_2} + \dots + \omega_{q_n})t} \tag{3.14}$$

According to expression (3.8) and summing equation (3.14) over n , $n=1,2,\dots,\infty$, the output of the nonlinear system can be obtained.

Fig. 3.2 shows the Volterra series representation of a nonlinear system. A nonlinear transfer function can be treated as a transformation function which transforms an input signal to an output signal in the order of the nonlinear transfer function. Output of the nonlinear system is a summation of responses from different

nonlinear transfer functions. In order to have a complete description of the nonlinear output, index n should be infinite or tend to infinite. For the sake of analysis, weakly nonlinear approximation is usually adopted and nonlinear transfer functions with order higher than 3 are truncated. The definition of “weakly nonlinear” is explained in the followed section.

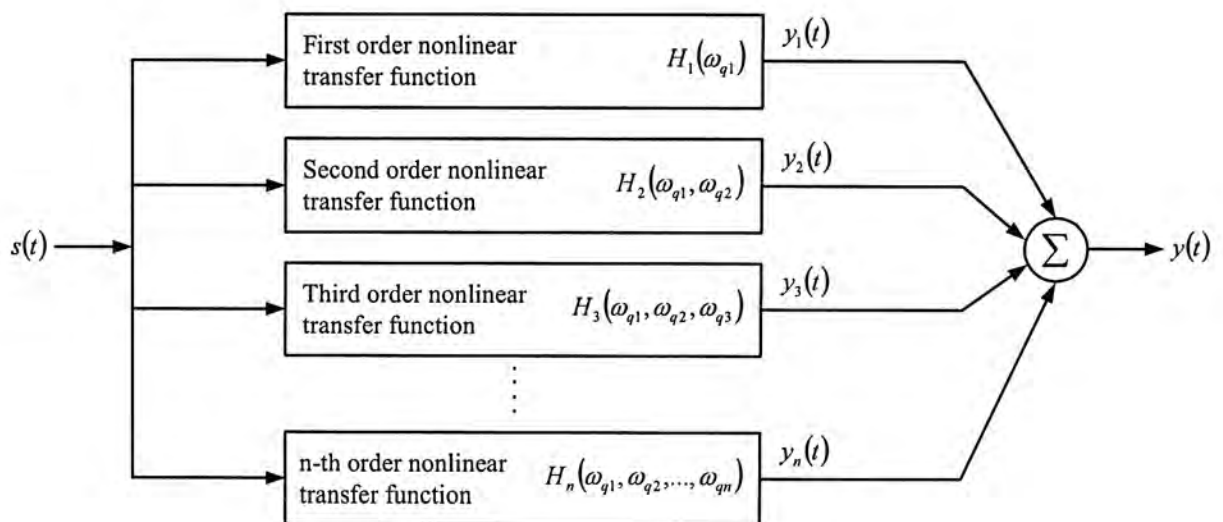


Fig. 3.2 Volterra series representation of nonlinear system

3.3 Weakly Nonlinear Approximation

Recall expression (3.8) and (3.14), output of any nonlinear system can be described by:

$$y(t) = \sum_{n=1}^{\infty} y_n(t) \quad (3.15)$$

where

$$y_n(t) = \frac{1}{2^n} \sum_{\substack{q_1=-Q \\ q_1 \neq 0}}^Q \sum_{\substack{q_2=-Q \\ q_2 \neq 0}}^Q \dots \sum_{\substack{q_n=-Q \\ q_n \neq 0}}^Q H_n(\omega_{q_1}, \omega_{q_2}, \dots, \omega_{q_n}) v_{s,q_1} v_{s,q_2} \dots v_{s,q_n} e^{j(\omega_{q_1} + \omega_{q_2} + \dots + \omega_{q_n})t} \quad (3.16)$$

If the strength of the excitation is sufficiently small, the output can be described by considering only the first-order response of the system, represented by $H_1(\)$ which is actually the transfer function of the linearized system. The system behaves weakly nonlinearly when the strength of the excitation increases to a region at where the second- and third-order nonlinear responses have to be taken into consideration, which are modeled by $H_2(\)$ and $H_3(\)$. The overall output is the sum of responses from the first three nonlinear transfer functions. In terms of Volterra series, a system behaves weakly nonlinearly if, for the applied input excitation, the output response can be accurately described by the first three nonlinear transfer functions. Even though the error involved may be up to a few dB, weakly nonlinear approximation can still be applied if the results obtained yield insight in the system's nonlinear behavior. Generally speaking, it is adequate to apply weakly nonlinear

approximation in the analysis of class A or class AB amplifiers that are operating a few dB backoff from 1dB gain compression point.

When strength of the excitation increase further, higher order nonlinear responses have to be included which are modeled by $H_n(\cdot)$ and the weakly nonlinear approximation is no longer valid.

3.4 Nonlinear Modeling

For analysis purposes, active devices are usually modeled by their equivalent circuit which may consist of both linear and nonlinear elements. Strictly speaking, solid state devices are not truly lumped, so any model is necessarily an approximation. Sophisticated nonlinear model are available [36, 37] for accurate representation. The I/V characteristics of nonlinear elements in the vicinity of the DC basing point, may be described by the Taylor series expansion.

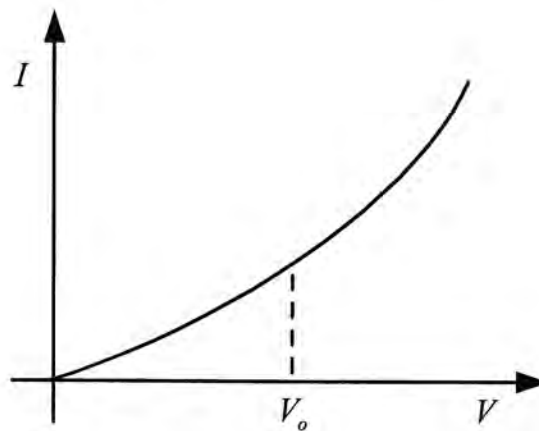


Fig. 3.3 A voltage controlled nonlinear element

Fig. 3.3 shows the I/V characteristic of a voltage controlled nonlinear element,

$I = f(V)$. A small deviation around the DC biasing point, V_o , can be modeled by,

$$\begin{aligned}
 i &= f(V_o + v) - f(V_o) \\
 &= \left. \frac{df(V)}{dV} v + \frac{1}{2} \frac{d^2 f(V)}{dV^2} v^2 + \frac{1}{6} \frac{d^3 f(V)}{dV^3} v^3 + \dots \right|_{\text{at } V = V_o}
 \end{aligned}
 \tag{3.17}$$

or

$$i = c_1 v + c_2 v^2 + c_3 v^3 + \dots \tag{3.18}$$

where c_n are the coefficients to be determined. Three typical nonlinear elements are

listed below:

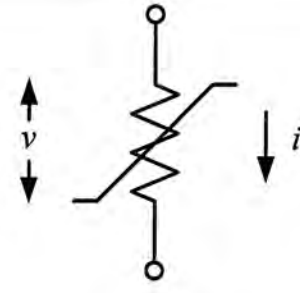
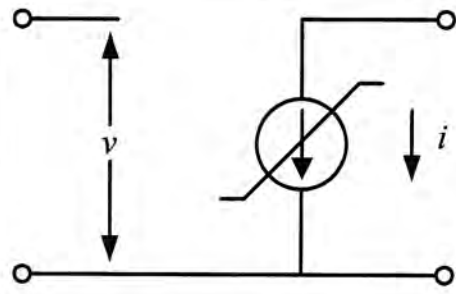
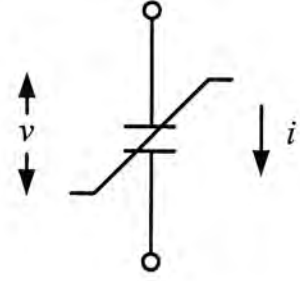
<p>Nonlinear conductance</p>		$i = g_1 v + g_2 v^2 + g_3 v^3 + \dots$
<p>Nonlinear transconductance</p>		$i = gm_1 v + gm_2 v^2 + gm_3 v^3 + \dots$
<p>Nonlinear capacitance</p>		$q = C_1 v + C_2 v^2 + C_3 v^3 + \dots$

Table 3.1 Nonlinear elements

Note that all the nonlinear coefficients, g_n , gm_n and C_n are bias dependent.

The indication of time dependence, (t) , have been deleted from $i(t)$ and $v(t)$ as usual manner. In the case of nonlinear capacitance, the charge-voltage relation can be converted to current-voltage relation by differentiating the expression with respect to time.

Fig. 3.4 shows a simplified nonlinear model of MESFET [37] which mainly comprises, the gate-to-source capacitance (C_{gs}), the drain-to-source transconductance (g_m) and the drain-to-source conductance (g_{ds}) [38].

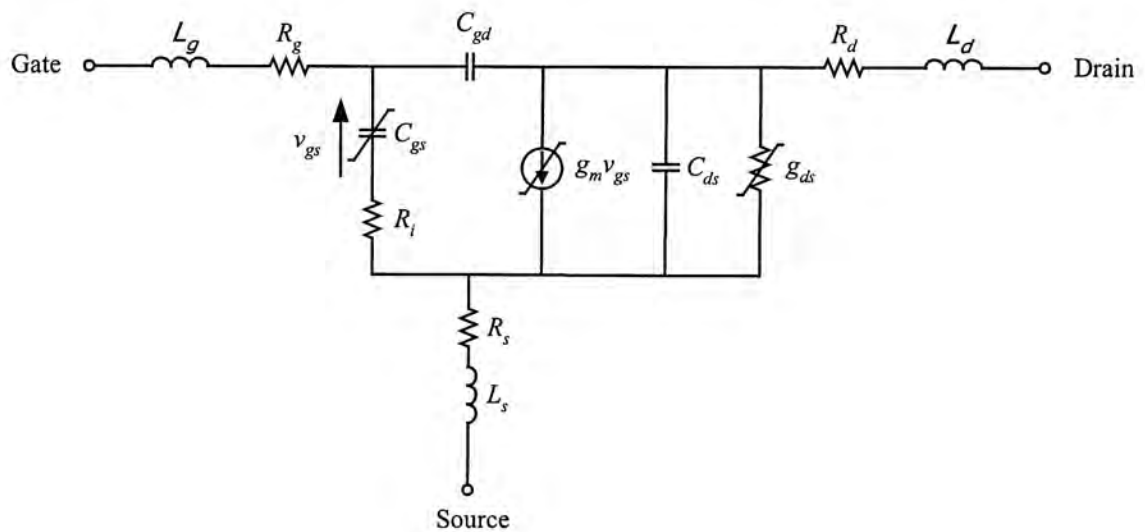


Fig. 3.4 Nonlinear model of MESFET

3.5 Determination of Nonlinear Transfer Function

Both harmonic-input method and method of nonlinear current can be adopted for determining the nonlinear transfer functions of a nonlinear system. The method of nonlinear current will be introduced here, as it is easier to use and more amenable to computer-aided design. Readers may refer to [38] for the details of harmonic-input method.

For the purpose of illustration, consider a system which contains a voltage source, a nonlinear resistor and a network composed of linear elements only.

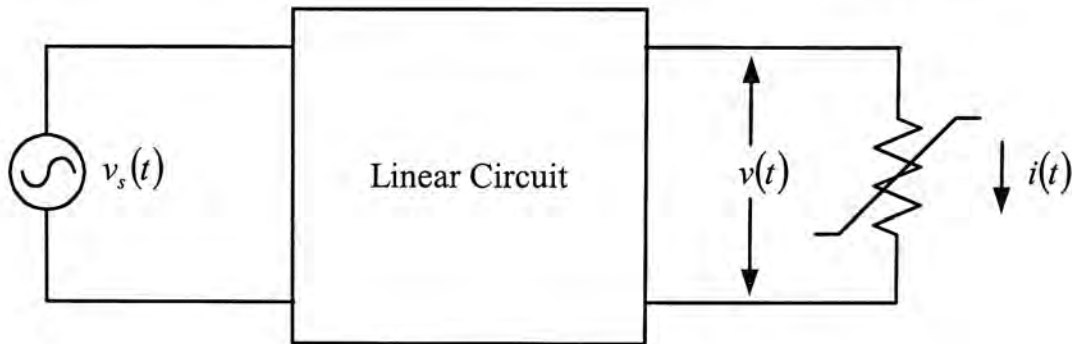


Fig. 3.5 System including a nonlinear resistor

The nonlinear current is described by:

$$i(t) = g_1 v(t) + g_2 v^2(t) + g_3 v^3(t) + \dots \quad (3.19)$$

where g_n ($n=1,2,3$) is the biasing dependent coefficients of the nonlinear resistor.

The voltage $v(t)$ consists of all order of mixing products,

$$v(t) = v_1(t) + v_2(t) + v_3(t) + \dots \quad (3.20)$$

where $v_n(t)$ represents the sum of all n -th order mixing products. Substituting (3.20)

into (3.19) and grouping the mixing products of the same order, we have:

$$i_1(t) = g_1[v_1(t) + v_2(t) + v_3(t)] \quad (3.21)$$

$$i_2(t) = g_2 v_1^2(t) \quad (3.22)$$

$$i_3(t) = 2g_2 v_1(t)v_2(t) + g_3 v_1^3(t) \quad (3.23)$$

Mixing products with order higher than three are neglected as manner of weakly nonlinear approximation. Fig. 3.5 can be redrawn as:

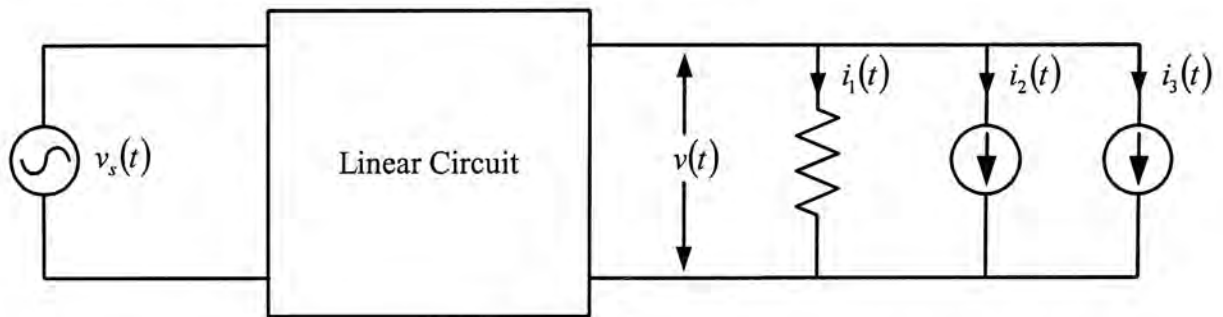


Fig. 3.6 Equivalent representation of system with a nonlinear conductance

The current sources $i_2(t)$ and $i_3(t)$ in Fig. 3.6 represents all the second- and third-order current components that are arose from the nonlinear coefficients in equation (3.19). Fig. 3.6 indicates that the system under consideration is linear, although the current sources are nonlinear functions of voltages at various orders. Moreover, Fig. 3.6 reveals that the first-order voltage component, $v_1(t)$, is generated by the source, $v_s(t)$. The second-order current, $i_2(t)$, is a function of the first-order voltages while the third-order current, $i_3(t)$, is a function of the first- and second-order voltages. The currents with order greater than one are always functions of lower-order voltages. In order to find the nonlinear transfer function, we can:

1. Find $v_1(t)$ by setting all the currents sources equal to 0 under the excitation of

$v_s(t)$. The first-order nonlinear transfer function can be determined by:

$$H_1(\omega_{q1}) = \frac{v_1(\omega_{q1})}{v_s(\omega_{q1})} \quad (3.24)$$

where $v_s(\omega_{q1})$ and $v_{q1}(\omega)$ denotes the Fourier transform of $v_s(t)$ and $v_s(t)$ respectively.

- From $v_1(t)$, the second-order current can be found, $i_2(t) = g_2 v_1^2(t)$. The second-order voltage, $v_2(t)$, can be found by setting $v_s(t)$ equal to 0 and $i_2(t)$ as the only excitation. The second-order nonlinear transfer function is given by:

$$H_2(\omega_{q1}, \omega_{q2}) = \frac{v_2(\omega_{q1}, \omega_{q2})}{v_s(\omega_{q1})v_s(\omega_{q2})} \quad (3.25)$$

- The third order current, $i_3(t)$, can be found from $v_1(t)$, $v_2(t)$, g_2 and g_3 , and with $v_s(t)$ and $i_2(t)$ set to 0. The third-order nonlinear transfer function is described by:

$$H_3(\omega_{q1}, \omega_{q2}, \omega_{q3}) = \frac{v_3(\omega_{q1}, \omega_{q2}, \omega_{q3})}{v_s(\omega_{q1})v_s(\omega_{q2})v_s(\omega_{q3})} \quad (3.26)$$

With the determined nonlinear transfer function $H_n(\)$, analyses of the system can be carried out. The frequency components of interest can be evaluated in a straightforward manner via expression (3.14).

Chapter 4 Manifestation of Nonlinear Behavior

Distortions in amplifiers are characterized by harmonic distortion, AM/AM, AM/PM and intermodulation distortion. In this chapter, the nonlinear behavior of a generic amplifier is analyzed by the Volterra series method as introduced in the previous chapter. The figures of merit for characterizing distortions as well as their impact on system performance are described.

4.1 Two-Tone Volterra Series Analysis

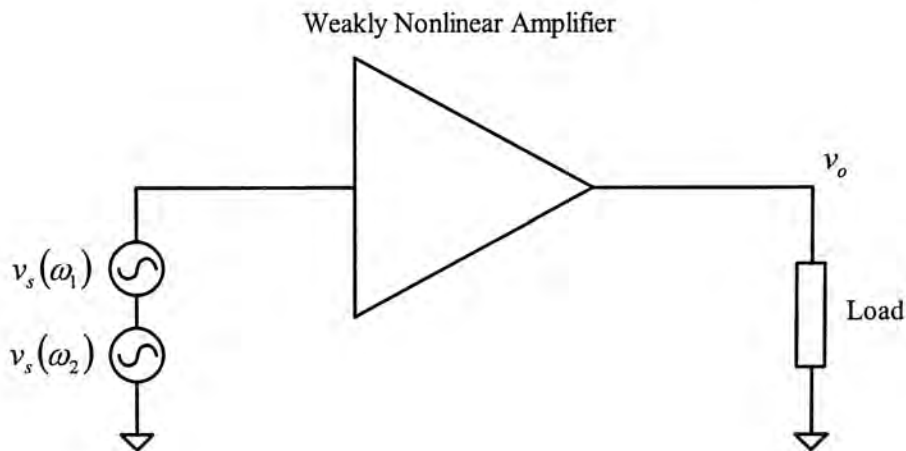


Fig. 4.1 A generic amplifier model under two-tone excitation

Fig. 4.1 shows the generic amplifier model under consideration. The amplifier is operating in weakly nonlinear region at where the output response can be accurately described by the first three nonlinear transfer functions. The excitation consists of two sinusoidal sources at angular frequency of ω_1 and ω_2 , both with strength of v_s . The first-, second- and third-order responses can be derived as:

$$v_1(t) = \frac{1}{2} \sum_{\substack{q1=-2 \\ q1 \neq 0}}^2 H_1(\omega_{q1}) v_s e^{j\omega_{q1}t} \quad (4.1)$$

$$v_2(t) = \frac{1}{4} \sum_{\substack{q1=-2 \\ q1 \neq 0}}^2 \sum_{\substack{q2=-2 \\ q2 \neq 0}}^2 H_2(\omega_{q1}, \omega_{q2}) v_s v_s e^{j(\omega_{q1} + \omega_{q2})t} \quad (4.2)$$

$$v_3(t) = \frac{1}{8} \sum_{\substack{q1=-2 \\ q1 \neq 0}}^2 \sum_{\substack{q2=-2 \\ q2 \neq 0}}^2 \sum_{\substack{q3=-2 \\ q3 \neq 0}}^2 H_3(\omega_{q1}, \omega_{q2}, \omega_{q3}) v_s v_s v_s e^{j(\omega_{q1} + \omega_{q2} + \omega_{q3})t} \quad (4.3)$$

where $H_n(\)$, $n=1,2,3$, are the n -th order nonlinear transfer function between the excitation and load. All the possible frequency components generated are tabulated in Table. 4.1.

For single tone excitation, either $v_s(\omega_1)$ or $v_s(\omega_2)$ can be set to 0. Note that beside the input signal at angular frequencies ω_1 and ω_2 are being amplified.

There are three main types of distortion generated, they are

1. Harmonic distortion
2. AM/AM and AM/PM distortion
3. Intermodulation distortion

Frequency	Amplifier output
0	$\frac{1}{2}H_2(\omega_1, -\omega_1)v_s(\omega_1)v_s(-\omega_1)$ $+ \frac{1}{2}H_2(\omega_2, -\omega_2)v_s(\omega_2)v_s(-\omega_2)$
$\omega_2 - \omega_1$	$H_2(\omega_2, -\omega_1)v_s(\omega_2)v_s(-\omega_1)$
$2\omega_1 - \omega_2$	$\frac{3}{4}H_3(\omega_1, \omega_1, -\omega_2)v_s(\omega_1)v_s(\omega_1)v_s(-\omega_2)$
ω_1	$H_1(\omega_1)v_s(\omega_1) + \frac{3}{4}H_3(\omega_1, \omega_1, -\omega_1)v_s(\omega_1)v_s(\omega_1)v_s(-\omega_1)$ $+ \frac{3}{2}H_3(\omega_1, \omega_2, -\omega_2)v_s(\omega_1)v_s(\omega_2)v_s(-\omega_2)$
ω_2	$H_1(\omega_2)v_s(\omega_2) + \frac{3}{4}H_3(\omega_2, \omega_2, -\omega_2)v_s(\omega_2)v_s(\omega_2)v_s(-\omega_2)$ $+ \frac{3}{2}H_3(\omega_2, \omega_1, -\omega_1)v_s(\omega_2)v_s(\omega_1)v_s(-\omega_1)$
$2\omega_2 - \omega_1$	$\frac{3}{4}H_3(\omega_2, \omega_2, -\omega_1)v_s(\omega_2)v_s(\omega_2)v_s(-\omega_1)$
$2\omega_1$	$\frac{1}{2}H_2(\omega_1, \omega_1)v_s(\omega_1)v_s(\omega_1)$
$\omega_1 + \omega_2$	$H_2(\omega_1, \omega_2)v_s(\omega_1)v_s(\omega_2)$
$2\omega_2$	$\frac{1}{2}H_2(\omega_2, \omega_2)v_s(\omega_2)v_s(\omega_2)$
$3\omega_1$	$\frac{1}{4}H_3(\omega_1, \omega_1, \omega_1)v_s(\omega_1)v_s(\omega_1)v_s(\omega_1)$
$2\omega_1 + \omega_2$	$\frac{3}{4}H_3(\omega_1, \omega_1, \omega_2)v_s(\omega_1)v_s(\omega_1)v_s(\omega_2)$
$\omega_1 + 2\omega_2$	$\frac{3}{4}H_3(\omega_2, \omega_2, \omega_1)v_s(\omega_2)v_s(\omega_2)v_s(\omega_1)$
$3\omega_2$	$\frac{1}{4}H_3(\omega_2, \omega_2, \omega_2)v_s(\omega_2)v_s(\omega_2)v_s(\omega_2)$

Table 4.1 Output of weakly nonlinear amplifier under two-tone excitation

4.2 Harmonic Distortion

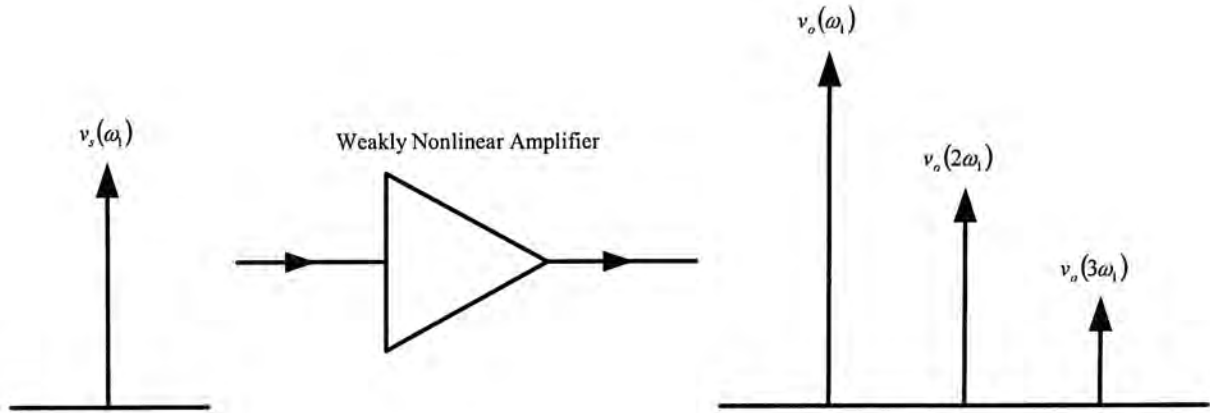


Fig. 4.2 Generation of harmonic distortions

When amplifier is driven into weakly nonlinear region by a single sinusoidal signal at angular frequency ω_1 . Distortions at harmonic frequencies are generated and value of the n -th harmonic is given by

$$v_o(n\omega_1) = \frac{1}{2^{n-1}} H_n(\omega_1, \omega_1, \dots, \omega_1) v_s^n(\omega_1) \quad (4.4)$$

For example, the second harmonic component is

$$v_o(2\omega_1) = \frac{1}{2} H_n(\omega_1, \omega_1) v_s(\omega_1) v_s(\omega_1) \quad (4.5)$$

and the third harmonic component is

$$v_o(3\omega_1) = \frac{1}{4} H_n(\omega_1, \omega_1, \omega_1) v_s(\omega_1) v_s(\omega_1) v_s(\omega_1) \quad (4.6)$$

Harmonic distortions are of the least concern as they are at least one carrier frequency far apart from the desired in-band signal. Harmonic distortion can be filtered out by harmonic filter.

4.3 AM/AM and AM/PM

AM/AM and AM/PM account for the distortion components generated at the same frequency as the input signal. For single tone excitation at angular frequency ω_1 , the output at the same frequency is given by:

$$v_o(\omega_1) = H_1(\omega_1)v_s(\omega_1) + \frac{3}{4}H_3(\omega_1, \omega_1, -\omega_1)v_s(\omega_1)v_s(\omega_1)v_s(-\omega_1) \quad (4.7)$$

Defining gain of the system as the ratio of total output to input:

$$g(\omega_1) = \frac{v_o(\omega_1)}{v_s(\omega_1)} \quad (4.8)$$

Substituting (4.7) into (4.8) gives:

$$g(\omega_1) = H_1(\omega_1) + \frac{3}{4}H_3(\omega_1, \omega_1, -\omega_1)v_s(\omega_1)v_s(-\omega_1) \quad (4.9)$$

For amplifiers, the sign of $H_3(\omega_1, \omega_1, -\omega_1)$ is always negative. Hence, when input power increases, gain of amplifier decreases. Equation (4.9) also indicates that $g(\omega_1)$ can be expressed as the sum of two phasor, as shown in Fig. 4.3.

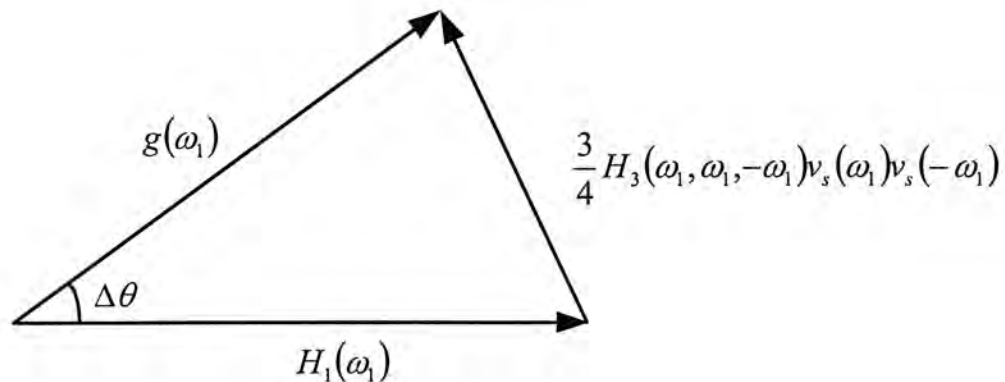


Fig. 4.3 AM/AM and AM/PM phenomenon

As $v_s(\omega_1)$ increases, both magnitude and phase of $g(\omega_1)$ change. The change in

magnitude of $g(\omega_1)$ is called AM/AM distortion while the change in phase of $g(\omega_1)$ is known as AM/PM distortion. For linear modulation formats such as QPSK and QAM, AM/AM and AM/PM phenomenon cause shifting of signaling points in the constellation diagram. Hence fidelity of the transmitted signal is impaired and bit error rate of the system is increased.

As explained before, gain of amplifier decreases as input power increases. The output power level at where the gain is compressed by 1dB is termed as 1dB gain compression point (P_{1dB}). P_{1dB} is usually used as a figure of merit to specify the power capability of an amplifier (Fig. 4.4).

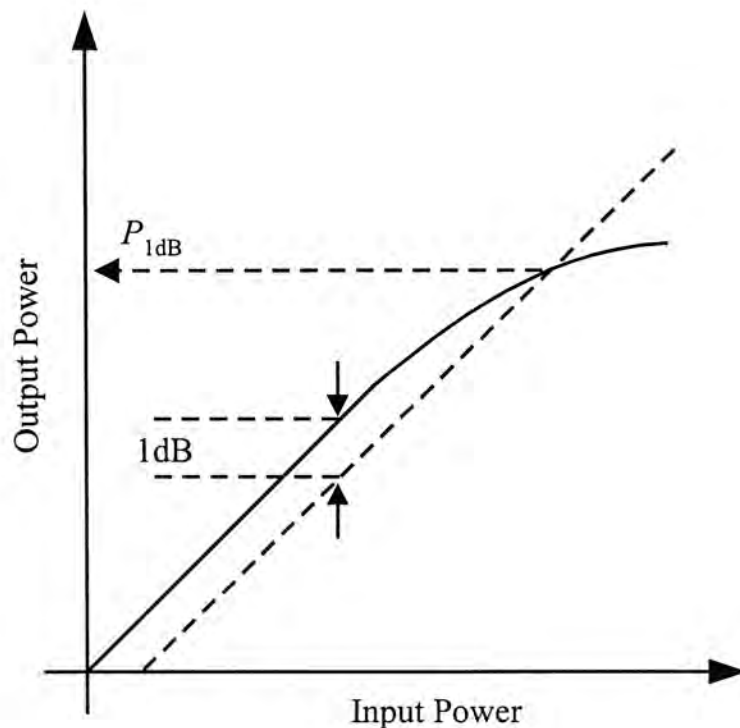


Fig. 4.4 Definition of P_{1dB}

4.4 Intermodulation Distortion

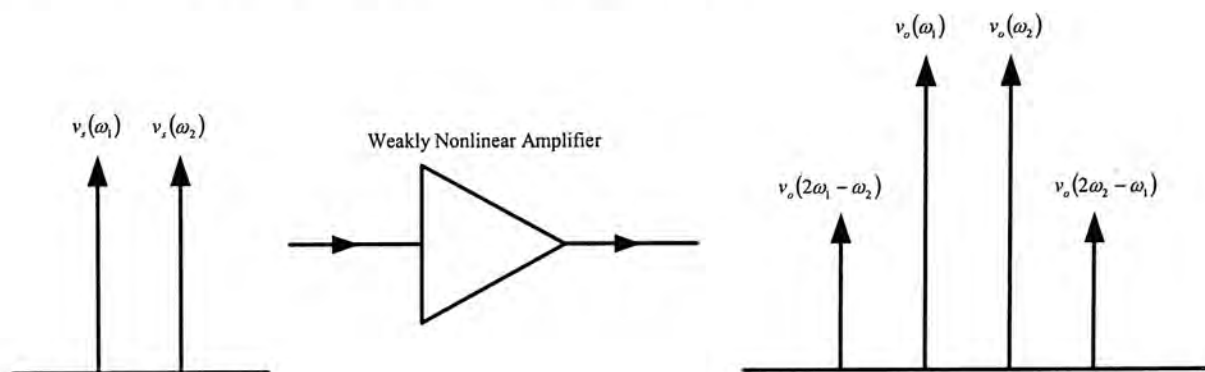


Fig. 4.5 Generation of intermodulation distortion

Unlike the AM/AM, AM/PM and harmonic distortion, intermodulation distortion occurs only in the case of multi-tone excitation. Intermodulation distortion is caused by the mixing of signals through the odd-order nonlinear transfer functions. If the excitation contains frequency components at ω_1 and ω_2 , intermodulation distortion components at $2\omega_1 - \omega_2$ and $2\omega_2 - \omega_1$ are generated:

$$v_o(2\omega_1 - \omega_2) = \frac{3}{4} H_3(\omega_1, \omega_1, -\omega_2) v_s(\omega_1) v_s(\omega_1) v_s(-\omega_2) \quad (4.10)$$

$$v_o(2\omega_2 - \omega_1) = \frac{3}{4} H_3(\omega_2, \omega_2, -\omega_1) v_s(\omega_2) v_s(\omega_2) v_s(-\omega_1) \quad (4.11)$$

Note that intermodulation distortion is very close to the fundamental signal tones and cannot be eliminated by filtering techniques. The IMD performance of amplifier is crucial in many communication systems as it can create undesired interference in adjacent channels. It is noted that intermodulation distortion, AM/AM and AM/PM distortion are arose from the same source, the third order nonlinear transfer function

or third order nonlinearities presented in the system. With intermodulation distortion being suppressed, AM/AM and AM/PM are also being improved, vice versa.

Two-tone test is a widely accepted method for assessing amplifier linearity. A common figure of merit to characterize amplifier linearity under two-tone excitation is the carrier-to-intermodulation ratio (C/I), in unit dBc, as illustrated in Fig. 4.6.

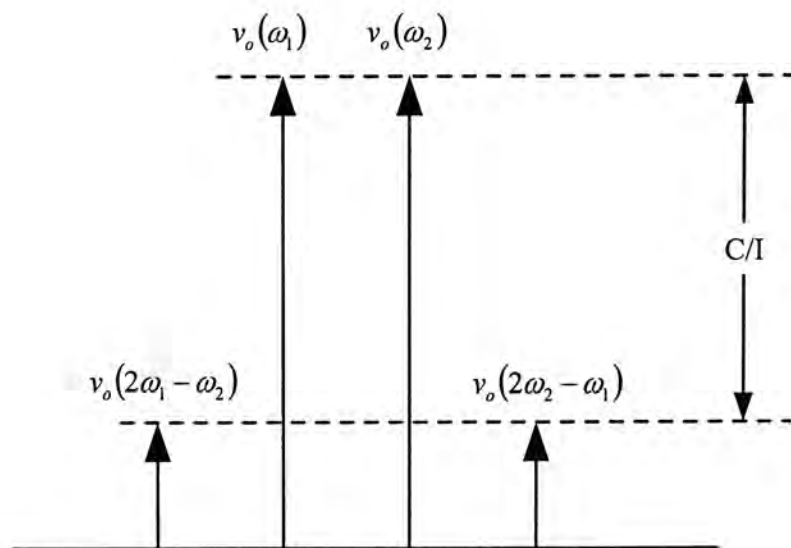


Fig. 4.6 Definition of carrier-to-intermodulation ratio

Chapter 5 The Generalized Baseband Signal Injection Method

This chapter starts by the investigation of conventional difference-frequency (baseband) signal injection method. Limitations of the method are identified and a new linearization method, the generalized baseband signal injection method, is then proposed. Mathematical formulations of the proposed method are detailed by using the concept of Volterra series as described previously. Moreover, the application of the new technique to the linearization of predistorter-amplifier and multi-stage amplifier configurations are demonstrated. Furthermore, the operating conditions for optimal IMD suppression of the proposed method are also developed. In contrast to many linearization methods, the proposed method can achieve higher linearity performance and is simpler and less expensive to implement. No RF circuitry such as variable gain amplifiers and phase shifters are needed other than baseband amplifiers.

5.1 Generalized Baseband Signal Injection Method (GM)

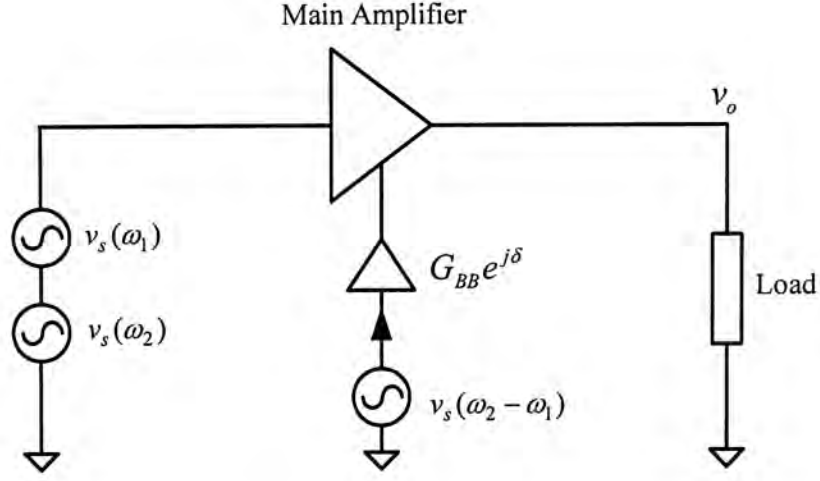


Fig. 5.1 Conventional baseband signal injection method

Fig. 5.1 shows the basic configuration of the conventional baseband signal injection method [39, 40]. The main amplifier to be linearized is constructed by using solid state active devices such as FET or BJT. The baseband signal ($\omega = \omega_2 - \omega_1$) may be injected into the amplifier through the biasing circuitry. Using Volterra Series notation, the output IMD component of the amplifier may be expressed as:

$$v_o(2\omega_1 - \omega_2) = \frac{3}{4} H_3(\omega_1, \omega_1, -\omega_2) v_s(\omega_1) v_s(\omega_1) v_s(-\omega_2) + H_2(\omega_1 - \omega_2, \omega_1) G_{BB} e^{-j\delta} v_s(\omega_1 - \omega_2) v_s(\omega_1) \quad (5.1)$$

$$v_o(2\omega_2 - \omega_1) = \frac{3}{4} H_3(\omega_2, \omega_2, -\omega_1) v_s(\omega_2) v_s(\omega_2) v_s(-\omega_1) + H_2(\omega_2 - \omega_1, \omega_2) G_{BB} e^{j\delta} v_s(\omega_2 - \omega_1) v_s(\omega_2) \quad (5.2)$$

where $H_n(\)$ represent the n -order nonlinear transfer function of the main amplifier; G_{BB} is the voltage gain of the baseband amplifier required for the injection and δ denotes the phase shift associated with the baseband amplifier. The relationship

between the input tones and the baseband signal is expressed as:

$$v_s(\omega_2 - \omega_1) = K_2(\omega_2, -\omega_1)v_s(\omega_2)v_s(-\omega_1) \quad (5.3)$$

where $K_2(\)$ denotes the second-order nonlinear transfer function of the injection signal generation circuitry.

Equation (5.1) and (5.2) indicates that the injected signal interacts with the fundamental component via the second-order nonlinear transfer function to produce new components at $\omega = 2\omega_1 - \omega_2$ and $\omega = 2\omega_2 - \omega_1$. In addition, as the baseband signal at $\omega_2 - \omega_1$ and $\omega_1 - \omega_2$ are complex conjugate pair: $\angle v_s(\omega_2 - \omega_1) = \delta$, and $\angle v_s(\omega_1 - \omega_2) = -\delta$.

Hence, equation (5.1) may be re-expressed as:

$$\begin{aligned} v_o(2\omega_2 - \omega_1) &= d_R \cdot v_s(\omega_2)v_s(\omega_2)v_s(-\omega_1) \\ &= [a e^{j\theta} + G_{BB} b e^{j\phi} e^{j\delta}] v_s(\omega_2)v_s(\omega_2)v_s(-\omega_1) \end{aligned} \quad (5.4)$$

where

$$a e^{j\theta} = \frac{3}{4} H_3(\omega_2, \omega_2, -\omega_1) \quad (5.5)$$

$$b e^{j\phi} = H_2(\omega_2 - \omega_1, \omega_2) K_2(\omega_2, -\omega_1) \quad (5.6)$$

Assuming that $\omega_1 \approx \omega_2$, the IMD component at $2\omega_1 - \omega_2$ may also be re-written as:

$$\begin{aligned} v_o(2\omega_1 - \omega_2) &= d_L \cdot v_s(\omega_1)v_s(\omega_1)v_s(-\omega_2) \\ &\approx [a e^{j\theta} + G_{BB} b e^{j\phi} e^{-j\delta}] v_s(\omega_1)v_s(\omega_1)v_s(-\omega_2) \end{aligned} \quad (5.7)$$

Fig. 5.2 illustrates the phasor representation of d_R and d_L .

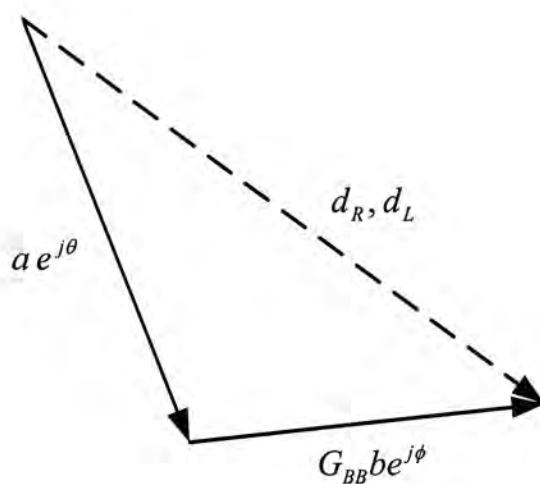
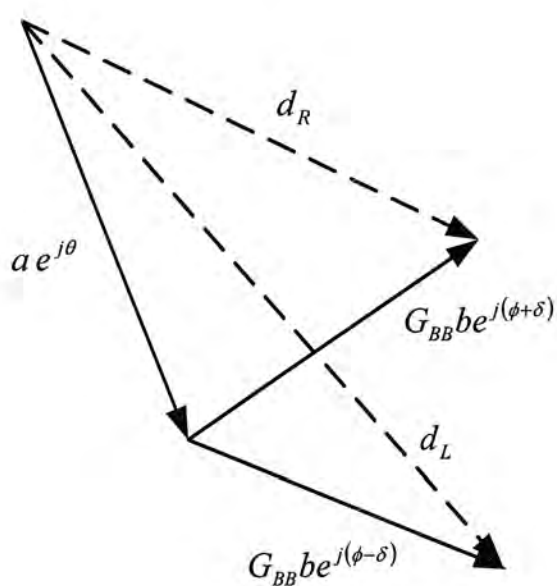
(a) $\delta = 0$ or π (b) $\delta \neq 0$ and π

Fig. 5.2 Phasor representation of conventional baseband signal injection method

Note that only amplitude of the injected signal ($G_{BB}b$) may be adjusted in the conventional approach. If $\delta \neq 0$ and π , IMD asymmetry occurs. Moreover, the diagram also reveals that, unless $\theta = \phi$ or $\theta = \phi + \pi$, the above mentioned injection method can only provide partial cancellation of the inherent IMD, and the improvement is limited. For complete suppression of IMD, the generalized baseband

injection method is proposed.

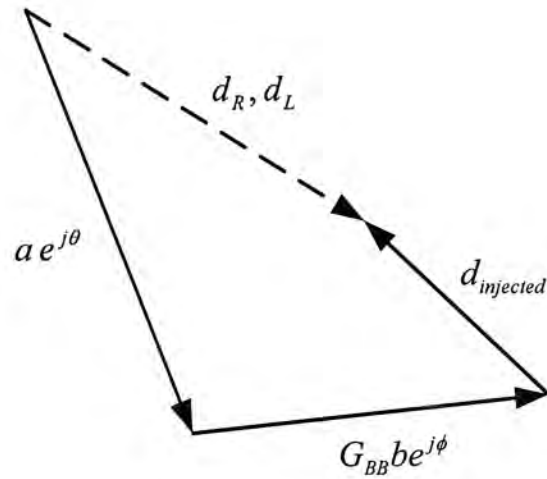


Fig. 5.3 Generalized baseband signal injection method

Fig. 5.3 illustrates the phasor representation of the generalized baseband signal injection method. An additional canceling signal ($d_{injected}$) is introduced to the circuit. In principle, this component can also be generated from the baseband signal source. Under these circumstances, the IMD product may be eliminated entirely by properly setting the strengths of the two vectors ($G_{BB} b e^{j\phi}$ and $d_{injected}$). Applications of the generalized baseband signal injection method to practical systems are detailed in the next section.

5.2 Application of GM to Predistorter-Amplifier

Linearization

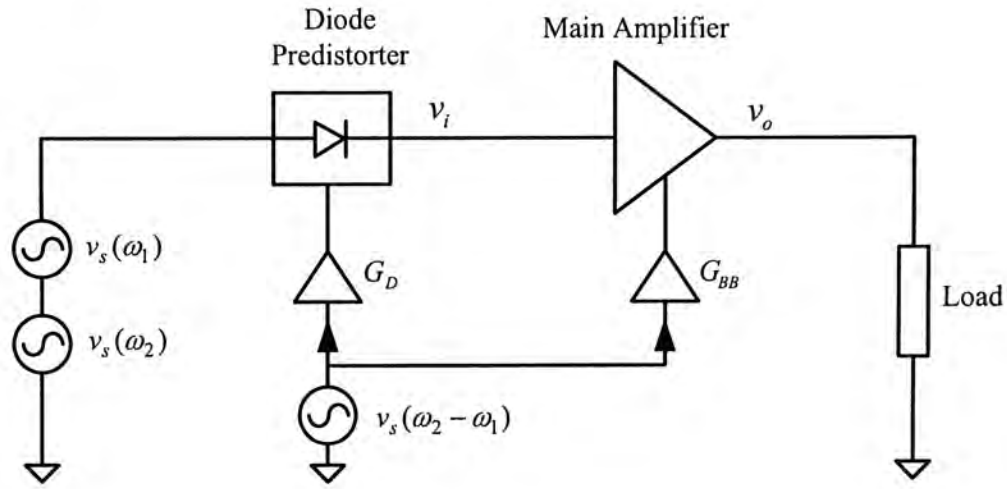


Fig. 5.4 Linearization of predistorter-amplifier system

Fig. 5.4 shows the practical realization of the generalized baseband injection method which consists of a diode predistorter in cascaded with the main amplifier.

The output voltage components of the diode predistorter can be written as:

$$v_i(\omega_1) = D_1(\omega_1)v_s(\omega_1) \quad (5.8)$$

$$v_i(\omega_2) = D_1(\omega_2)v_s(\omega_2) \quad (5.9)$$

$$v_i(2\omega_2 - \omega_1) = \frac{3}{4}D_3(\omega_2, \omega_2, -\omega_1)v_s(\omega_2)v_s(\omega_2)v_s(-\omega_1) + D_2(\omega_2 - \omega_1, \omega_2)G_D v_s(\omega_2 - \omega_1)v_s(\omega_2) \quad (5.10)$$

where $D_n(\)$ is the n -th order nonlinear transfer function of the diode predistorter;

G_D represents that the voltage gain of the baseband amplifier. Subsequently, the

third-order IMD component generated by the diode predistorter can be re-expressed

by:

$$v_i(2\omega_2 - \omega_1) = G_{IMD} e^{j\alpha} \cdot v_s(\omega_2) v_s(\omega_2) v_s(-\omega_1) \quad (5.11)$$

where

$$G_{IMD} e^{j\alpha} = \frac{3}{4} D_3(\omega_2, \omega_2, -\omega_1) + D_2(\omega_2 - \omega_1, \omega_2) G_D K_2(\omega_2, -\omega_1) \quad (5.12)$$

Note that by adjusting the polarity and magnitude of G_D , the value of G_{IMD} may be changed. Similarly, the third-order IMD component at $2\omega_1 - \omega_2$ can be derived as:

$$\begin{aligned} v_i(2\omega_1 - \omega_2) = & \frac{3}{4} D_3(\omega_1, \omega_1, -\omega_2) v_s(\omega_1) v_s(\omega_1) v_s(-\omega_2) \\ & + D_2(\omega_1 - \omega_2, \omega_1) G_D v_s(\omega_1 - \omega_2) v_s(\omega_1) \end{aligned} \quad (5.13)$$

Finally, the output IMD component of the main amplifier at $\omega = 2\omega_2 - \omega_1$ and $\omega = 2\omega_1 - \omega_2$ are given by:

$$\begin{aligned} v_o(2\omega_2 - \omega_1) = & \frac{3}{4} H_3(\omega_2, \omega_2, -\omega_1) v_i(\omega_2) v_i(\omega_2) v_i(-\omega_1) \\ & + H_2(\omega_2 - \omega_1, \omega_2) G_{BB} v_s(\omega_2 - \omega_1) v_i(\omega_2) \\ & + H_1(2\omega_2 - \omega_1) v_i(2\omega_2 - \omega_1) \end{aligned} \quad (5.14)$$

$$\begin{aligned} v_o(2\omega_1 - \omega_2) = & \frac{3}{4} H_3(\omega_1, \omega_1, -\omega_2) v_i(\omega_1) v_i(\omega_1) v_i(-\omega_2) \\ & + H_2(\omega_1 - \omega_2, \omega_1) G_{BB} v_s(\omega_1 - \omega_2) v_i(\omega_1) \\ & + H_1(2\omega_1 - \omega_2) v_i(2\omega_1 - \omega_2) \end{aligned} \quad (5.15)$$

By assuming that $\omega_1 \approx \omega_2$, expression (5.14) and (5.15) can be simplified as:

$$v_o(2\omega_1 - \omega_2) \approx v_o(2\omega_2 - \omega_1) = d \cdot v_s(\omega_2) v_s(\omega_2) v_s(-\omega_1) \quad (5.16)$$

where

$$d = a e^{j(\theta+\psi+\alpha)} + G_{BB} b e^{j(\phi+\psi+\alpha)} + c G_{IMD} e^{j(\psi+\alpha)} \quad (5.17)$$

$$\begin{aligned} a e^{j(\theta+\psi+\alpha)} = & \frac{3}{4} H_3(\omega_2, \omega_2, -\omega_1) D_1(\omega_2) D_1(\omega_2) D_1(-\omega_1) \\ \approx & \frac{3}{4} H_3(\omega_1, \omega_1, -\omega_2) D_1(\omega_1) D_1(\omega_1) D_1(-\omega_2) \end{aligned} \quad (5.18)$$

$$\begin{aligned}
be^{j(\phi+\psi+\alpha)} &= H_2(\omega_2 - \omega_1, \omega_2)D_1(\omega_2)K_2(\omega_2, -\omega_1) \\
&\approx H_2(\omega_1 - \omega_2, \omega_1)D_1(\omega_1)K_2(\omega_1, -\omega_2)
\end{aligned} \tag{5.19}$$

$$\begin{aligned}
ce^{j\psi} &= H_1(2\omega_2 - \omega_1) \\
&\approx H_1(2\omega_1 - \omega_2)
\end{aligned} \tag{5.20}$$

Inspection of equation (5.17) indicates that the output IMD component (d) may be totally suppressed with proper setting of G_{IMD} and G_{BB} values. For the sake of analysis, solutions of (5.17) can be sub-divided into 4 cases.

5.2.1 Case 1: Standalone Amplifier without Injection

In the absence of the diode predistorter and the injection of difference frequency signal ($G_{IMD} = 0$ and $G_{BB} = 0$), expression (5.17) is reduced to:

$$|d| = |a| \tag{5.21}$$

Magnitude of the distortion vector depends on the active device's nonlinearities, circuit impedances and topology adopted. Studies utilizing different forms of matching networks to improve linearity of amplifiers have been described in the literature [41-43]. In [44], the terminating impedances of the active devices at second-harmonic are optimized for improved linearity. The influences of doping profiles on MESFET IMD performance are also reported in [45, 46]. Nevertheless, improvement in IMD level that can be attained by these methods is limited.

5.2.2 Case 2: Injection to Amplifier Only

The conventional baseband signal injection method is obtained by setting $G_{IMD} = 0$ in (5.17), and the resulting expression for the third-order IMD becomes:

$$|d| = |ae^{j\theta} + G_{BB}be^{j\phi}| \quad (5.22)$$

Expression (5.22) shows that unless $\theta = \phi$ or $\theta = \phi + \pi$, this method can only achieve partial IMD cancellation. Moreover, condition for minimal IMD can be found by differentiating $|d|^2$ with respect to G_{BB} and equating the result to zero:

$$2a \cos(\theta)b \cos(\phi) + 2a \sin(\theta)b \sin(\phi) + 2G_{BB}b^2 = 0 \quad (5.23)$$

or

$$G_{BB} = \frac{-a \cos(\theta - \phi)}{b} \quad (5.24)$$

The corresponding level of IMD output is given by:

$$|d| = |a \sin(\theta - \phi)| \quad (5.25)$$

Note that in the case where $\theta - \phi = \pm \frac{\pi}{2}$, no IMD suppression is possible.

5.2.3 Case 3: Injection to Diode Predistorter Only

With baseband signal injected into the diode predistorter only ($G_{BB} = 0$), we have:

$$\begin{aligned} |d|^2 &= |ae^{j\theta} + cG_{IMD}|^2 \\ &= (a \cos \theta + cG_{IMD})^2 + a^2 \sin^2 \theta \end{aligned} \quad (5.26)$$

The optimum gain value for minimizing $|d|^2$ is thus given by:

$$G_{IMD} = \frac{-a \cos \theta}{c} \quad (5.27)$$

The corresponding residual IMD output is:

$$|d|^2 = a^2 \sin^2 \theta \quad (5.28)$$

Expression (5.26) indicates that only the in-phase distortion component can be removed and hence only partial cancellation of IMD is possible.

5.2.4 Case 4: Injection to Both Diode Predistorter and Amplifier

According to expression (5.17) and with injections to both the diode predistorter and amplifier, we have:

$$|d| = |ae^{j\theta} + G_{BB}be^{j\phi} + cG_{IMD}| \quad (5.29)$$

The requirements for complete cancellation are:

$$a \cos \theta + G_{BB}b \cos \phi + cG_{IMD} = 0 \quad (5.30)$$

$$a \sin \theta + G_{BB}b \sin \phi = 0 \quad (5.31)$$

The optimum condition for complete cancellation can be derived as:

$$G_{IMD} = \frac{a \sin(\theta - \phi)}{c \sin \phi} \quad (5.32)$$

$$G_{BB} = \frac{-a \sin \theta}{b \sin \phi} \quad (5.33)$$

Expression (5.32) and (5.33) reveals that, complete elimination of IMD can be achieved by varying the gain and polarity of the two baseband amplifiers.

5.3 Application of GM to Multi-Stage Amplifier Linearization

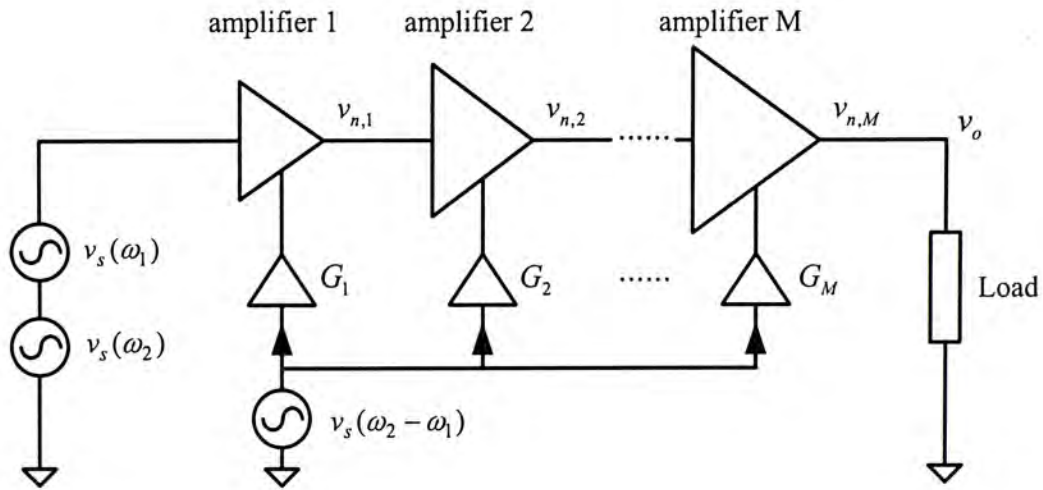


Fig. 5.5 Linearization of multi-stage amplifying system

In practice, the transmit path of RF front-end usually composes of a chain of cascaded amplifiers to achieve sufficient output power and signal gain. Fig. 5.5 shows the block diagram of the amplifying system under consideration. In the figure, there are M amplifiers, labeled as “amplifier 1” through “amplifier M ”. The mixing product generated by the individual nonlinear amplifier is denoted as $v_{n,m}$ where $m=1, 2, \dots, M$. It is also assumed that the injection signal at $\omega = \omega_2 - \omega_1$, is amplified and injected into the input of individual RF amplifier through the corresponding biasing networks.

Using the Volterra series notation and neglecting any mixing products higher than the third-order, the IMD components appearing at the output of “amplifier 1”

may be written as:

$$v_{3,1}(2\omega_1 - \omega_2) = \frac{3}{4}H_{3,1}(\omega_1, \omega_1, -\omega_2)v_s(\omega_1)v_s(\omega_1)v_s(-\omega_2) + H_{2,1}(\omega_1 - \omega_2, \omega_1)G_1v_s(\omega_1 - \omega_2)v_s(\omega_1) \quad (5.34)$$

$$v_{3,1}(2\omega_2 - \omega_1) = \frac{3}{4}H_{3,1}(\omega_2, \omega_2, -\omega_1)v_s(\omega_2)v_s(\omega_2)v_s(-\omega_1) + H_{2,1}(\omega_2 - \omega_1, \omega_2)G_1v_s(\omega_2 - \omega_1)v_s(\omega_2) \quad (5.35)$$

where $H_{n,m}(\)$ is the n -th order nonlinear transfer function of the m -th amplifier.

Note that the injection signal interacts with the fundamental via the second-order nonlinear function of the amplifier to generate a new component at $\omega = 2\omega_2 - \omega_1$.

The baseband signal is assumed to be generated by an external circuit. Without loss of generality, the relationship between the baseband signal and the input tones may be expressed as:

$$v_s(\omega_2 - \omega_1) = K_2(\omega_2, -\omega_1)v_s(\omega_2)v_s(-\omega_1) \quad (5.36)$$

where $K_2(\)$ denotes the second-order nonlinear transfer function of the baseband signal generation circuit. Subsequently, assuming that $\omega_2 \approx \omega_1$, equation (5.34) and (5.35) can be re-written as:

$$v_{3,1}(2\omega_1 - \omega_2) \approx v_{3,1}(2\omega_2 - \omega_1) = d_1 \cdot v_s(\omega_2)v_s(\omega_2)v_s(-\omega_1) \quad (5.37)$$

where

$$d_1 = a_1e^{j\theta_1} + G_1b_1e^{j\phi_1} \quad (5.38)$$

$$\begin{aligned} a_1e^{j\theta_1} &= \frac{3}{4}H_{3,1}(\omega_2, \omega_2, -\omega_1) \\ &\approx \frac{3}{4}H_{3,1}(\omega_1, \omega_1, -\omega_2) \end{aligned} \quad (5.39)$$

$$\begin{aligned} b_1 e^{j\phi} &= H_{2,1}(\omega_2 - \omega_1, \omega_2) K_2(\omega_2, -\omega_1) \\ &\approx H_{2,1}(\omega_1 - \omega_2, \omega_1) K_2(\omega_1, -\omega_2) \end{aligned} \quad (5.40)$$

Similarly, the IMD components generated by “amplifier 2” are therefore given by:

$$\begin{aligned} v_{3,2}(2\omega_1 - \omega_2) &= \frac{3}{4} H_{3,2}(\omega_1, \omega_1, -\omega_2) H_{1,1}(\omega_1) H_{1,1}(\omega_1) H_{1,1}(-\omega_2) v_s(\omega_1) v_s(\omega_1) v_s(-\omega_2) \\ &\quad + H_{2,2}(\omega_1 - \omega_2, \omega_1) G_2 v_s(\omega_1 - \omega_2) H_{1,1}(\omega_1) v_s(\omega_1) \end{aligned} \quad (5.41)$$

$$\begin{aligned} v_{3,2}(2\omega_2 - \omega_1) &= \frac{3}{4} H_{3,2}(\omega_2, \omega_2, -\omega_1) H_{1,1}(\omega_2) H_{1,1}(\omega_2) H_{1,1}(-\omega_1) v_s(\omega_2) v_s(\omega_2) v_s(-\omega_1) \\ &\quad + H_{2,2}(\omega_2 - \omega_1, \omega_2) G_2 v_s(\omega_2 - \omega_1) H_{1,1}(\omega_2) v_s(\omega_2) \end{aligned} \quad (5.42)$$

The above expression may be reduced to:

$$v_{3,2}(2\omega_1 - \omega_2) \approx v_{3,2}(2\omega_2 - \omega_1) = d_2 \cdot v_s(\omega_2) v_s(\omega_2) v_s(-\omega_1) \quad (5.43)$$

where

$$d_2 = a_2 e^{j\theta_2} + G_2 b_2 e^{j\phi_2} \quad (5.44)$$

$$\begin{aligned} a_2 e^{j\theta_2} &= \frac{3}{4} H_{3,2}(\omega_2, \omega_2, -\omega_1) H_{1,1}(\omega_2) H_{1,1}(\omega_2) H_{1,1}(-\omega_1) \\ &\approx \frac{3}{4} H_{3,2}(\omega_1, \omega_1, -\omega_2) H_{1,1}(\omega_1) H_{1,1}(\omega_1) H_{1,1}(-\omega_2) \end{aligned} \quad (5.45)$$

$$\begin{aligned} b_2 e^{j\phi_2} &= H_{2,2}(\omega_2 - \omega_1, \omega_2) K_2(\omega_2, -\omega_1) H_{1,1}(\omega_2) \\ &\approx H_{2,2}(\omega_1 - \omega_2, \omega_1) K_2(\omega_1, -\omega_2) H_{1,1}(\omega_1) \end{aligned} \quad (5.46)$$

In the general case, the IMD signal produced by “amplifier m ”, is simply equal to:

$$v_{3,m}(2\omega_1 - \omega_2) \approx v_{3,m}(2\omega_2 - \omega_1) = d_m \cdot v_s(\omega_2) v_s(\omega_2) v_s(-\omega_1) \quad (5.47)$$

where

$$d_m = a_m e^{j\theta_m} + G_m b_m e^{j\phi_m} \quad (5.48)$$

Consequently, the total IMD signal delivered to the load may thus be written as:

$$\begin{aligned}
 v_o(2\omega_1 - \omega_2) &\approx v_o(2\omega_2 - \omega_1) \\
 &= v_{3,1}(2\omega_2 - \omega_1) \cdot T_1 + \dots + v_{3,M-1}(2\omega_2 - \omega_1) \cdot T_{M-1} + v_{3,M}(2\omega_2 - \omega_1) \\
 &= d_M \cdot v_s(\omega_2)v_s(\omega_2)v_s(-\omega_1)
 \end{aligned} \tag{5.49}$$

where

$$T_m = \prod_{i=m+1}^M H_{1,i}(2\omega_2 - \omega_1) \tag{5.50}$$

$$\begin{aligned}
 d_M &= \left\{ a_M e^{j\theta_M} + a_{M-1} e^{j\theta_{M-1}} T_{M-1} + \dots + a_1 e^{j\theta_1} T_1 \right\} \\
 &\quad + \left\{ G_M b_M e^{j\phi_M} + G_{M-1} b_{M-1} e^{j\phi_{M-1}} T_{M-1} + \dots + G_1 b_1 e^{j\phi_1} T_1 \right\}
 \end{aligned} \tag{5.51}$$

It is clear from the above expression that the IMD signal may be viewed as the sum of two parts: the inherent IMD component (first bracket) generated by the amplifiers; and the canceling signal (second bracket) produced by the injection method. Inspection of (5.51) also indicates that the distortion component may be eliminated, with appropriate choices of the amplifier gains (G_m). The examination of different cases of signal injection and the corresponding conditions for optimum IMD suppression are presented in the following sections.

5.3.1 Case 1: Amplifying System with No Signal Injection

In the absence of any injection signal ($G_m = 0$), equation (5.51) can be re-expressed as:

$$\begin{aligned}
 |d_M| &= \left| a_M e^{j\theta_M} + a_{M-1} e^{j\theta_{M-1}} T_{M-1} + \dots + a_1 e^{j\theta_1} T_1 \right| \\
 &= \left| A e^{j\kappa} \right|
 \end{aligned} \tag{5.52}$$

The resultant vector, $A e^{j\kappa}$, represents the inherent IMD signal produced by the

composite amplifying system and may be used as a reference level for performance evaluation in the following sections.

5.3.2 Case 2: Amplifying System with Single Injection Point

From the implementation point of view, it is simpler to use only one injection signal. Under these circumstances, equation (5.51) may be written as:

$$|d_M| = \left| A e^{j\kappa} + G_p b_p e^{j\phi_p} T_p \right| \quad (5.53)$$

where p ($1 \leq p \leq M$) is the number of the amplifier stage associated with the injection point. Differentiating $|d_M|^2$ with respect to G_p and equating the result to zero gives:

$$2A \cos(\kappa) b_p |T_p| \cos(\phi + \angle T_p) + 2A \sin(\kappa) b_p |T_p| \sin(\phi + \angle T_p) + 2G_p b_p^2 |T_p|^2 = 0 \quad (5.54)$$

Consequently, the gain coefficient of the baseband amplifier for optimum IMD suppression can now be derived as:

$$G_p = \frac{-A \cos(\kappa - \phi_p - \angle T_p)}{b_p |T_p|} \quad (5.55)$$

The residual distortion can be evaluated by substituting (5.55) into (5.53),

$$|d_M| = \left| A \sin(\kappa - \phi_p - \angle T_p) \right| \quad (5.56)$$

Hence, the IMD suppression factor (dB) may be defined by:

$$-20 \log \left| \frac{d_M}{A} \right| = -20 \log \left| \sin(\kappa - \phi_p - \angle T_p) \right| \quad (5.57)$$

Equation (5.57) suggests that only partial cancellation of IMD is possible with single

point injection. The value of $(\kappa - \phi_p - \angle T_p)$ is normally non-zero and is a complex function of various device and circuit parameters.

5.3.3 Case 3: Amplifying System with Two Injection Points

In this case, an additional baseband signal is fed to the injection port of “amplifier q ”, and the corresponding expression for the resulting IMD output is therefore given by:

$$\begin{aligned} |d_M| &= \left| Ae^{j\kappa} + G_p b_p e^{j\phi_p} T_p + G_q b_q e^{j\phi_q} T_q \right| \\ &= \left| Ae^{j\kappa} + G_p b_p |T_p| e^{j\varphi_p} + G_q b_q |T_q| e^{j\varphi_q} \right| \end{aligned} \quad (5.58)$$

where $\varphi_p = \phi_p + \angle T_p$ and $\varphi_q = \phi_q + \angle T_q$. For optimum cancellation of the distortion signal, the following conditions must be satisfied,

$$A \cos \kappa + G_p b_p |T_p| \cos \varphi_p + G_q b_q |T_q| \cos \varphi_q = 0 \quad (5.59)$$

$$A \sin \kappa + G_p b_p |T_p| \sin \varphi_p + G_q b_q |T_q| \sin \varphi_q = 0 \quad (5.60)$$

or

$$G_p = \frac{-A}{b_p |T_p|} \cdot \frac{\sin(\kappa - \varphi_q)}{\sin(\varphi_p - \beta)} \quad (5.61)$$

$$G_q = \frac{A}{b_q |T_q|} \cdot \frac{\sin(\kappa - \varphi_p)}{\sin(\varphi_p - \varphi_q)} \quad (5.62)$$

The above expressions reveal that, in the presence of the second injection signal, it is possible to totally eliminate the IMD signal by properly adjusting the gains (G_p and G_q) of the baseband amplifiers. Equations (5.61) and (5.62) indicate that the gain

coefficients are real with either positive or negative sign, and therefore only constant gain amplifiers are required to maintain a low distortion output. In order to minimize the required gain values (G_p and G_q), the two injection points should be selected such that $|\varphi_p - \varphi_q| \approx \frac{\pi}{2}$, if possible.

Chapter 6 Experimental Setup and Measurements

In the previous chapters, it is shown that third-order IMD can be significantly suppressed by using the generalized baseband signal injection technique. For experimental verification, two amplifying systems operating at approximately 2GHz have been designed and constructed. In this chapter, the design and construction are of the systems are described in detail. Both two-tone and vector signal are employed for characterizing the IMD performances of both systems. For two-tone test, signals centered at 2GHz with frequency spacing of 100KHz are used. For the vector signal measurement, standard PHS signal ($\pi/4$ DQPSK modulated signal with data rate of 384Kbit/s) is employed.

In modern communication systems, power control strategy is usually adopted to reduce unwanted interference and power consumption. Conventionally, lookup table [47, 48] or adaptive techniques [49, 50] are often employed to maintain a low distortion output over a wide range of output power level. These approaches offer different degree of linearity performance at the expense of circuit complexity. The dynamic range of the proposed method is addressed.

6.1 Experimental Setup

The major hardware required for setting up the experiments are listed below:

	Experiment 1	Experiment 2
Diode predistorter	√	
Small signal amplifier	√	√
Medium power amplifier		√
Baseband signal generation circuit	√	√
Baseband amplifiers	√	√

Table 6.1 The experimental hardware

6.1.1 Diode Predistorter

Fig. 6.1 shows the schematic diagram of the diode predistorter. The diode used is Schottky diode SMS7621 from Alpha Industries. Both the biasing voltage and the baseband signal are fed to the diode circuitry through the biasing network. RF signals are isolated from the low-frequency circuitry by using quarter-wavelength microstrips and radial stubs. The large radial stub provides a good RF short at the fundamental while the small radial stub presents a short-circuit termination at the second-harmonic. The substrate used is FR4 with thickness of 0.8mm and $\epsilon_r = 4.4$.

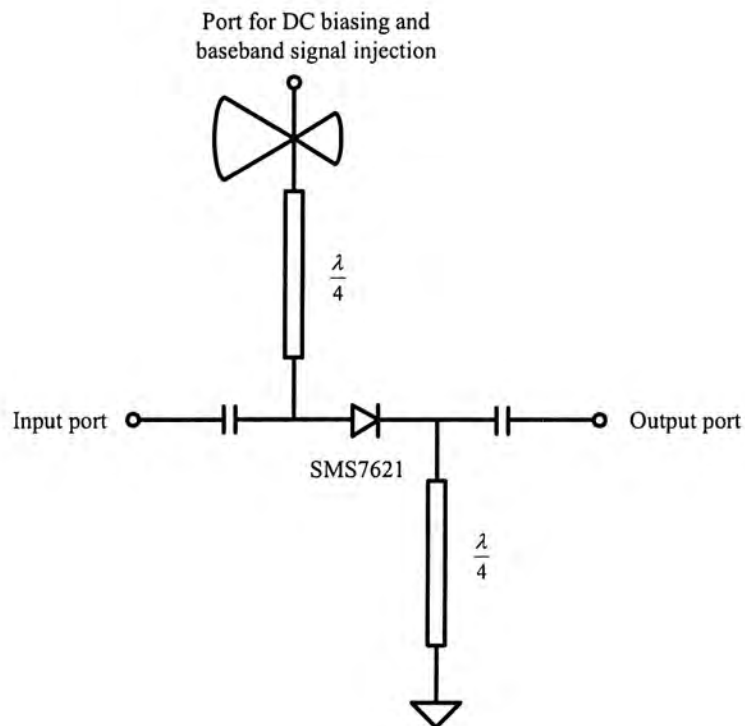


Fig. 6.1 Schematic of the diode predistorter

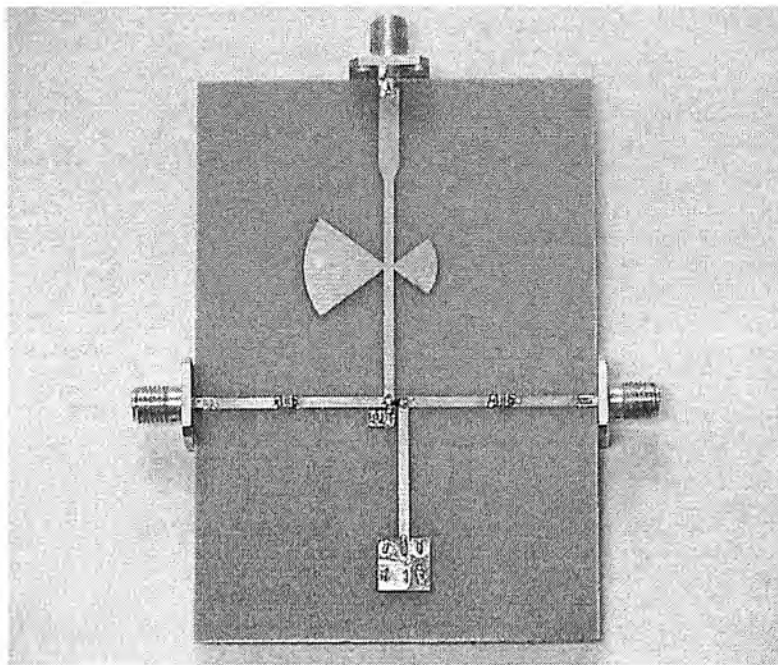


Fig. 6.2 Diode predistorter constructed

Fig. 6.2 shows the physical view of the diode predistorter. The transmission and reflection coefficients of the diode predistorter are measured using Advantest

network analyzer R3767CG and plotted in Fig. 6.3. Insertion loss of the predistorter is found to be 2dB. The input return loss is better than 10dB and the output return loss is better than 20dB.

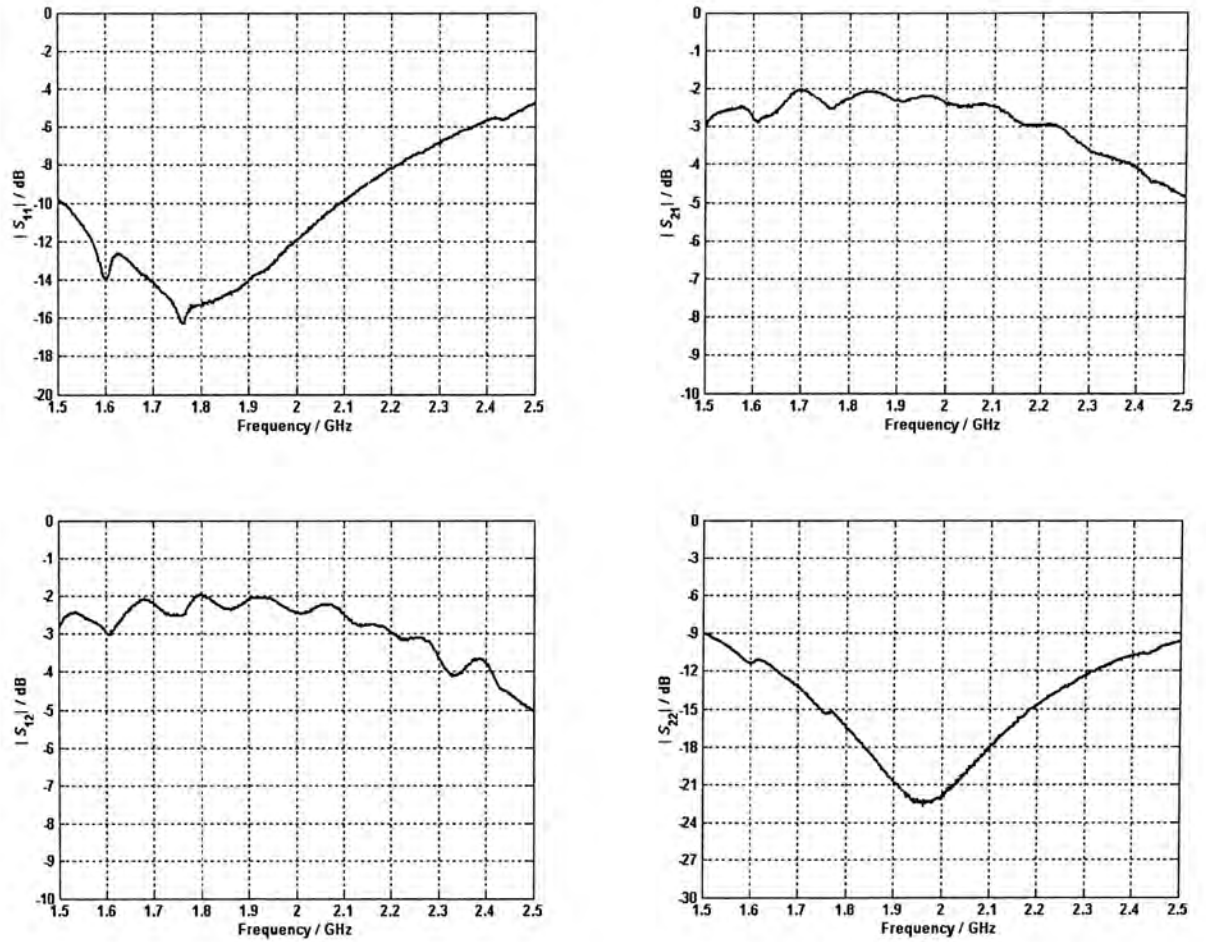


Fig. 6.3 S -parameter of the diode predistorter

Fig. 6.4 shows the output IMD level of the diode predistorter versus the strength of the baseband injection signal. The fundamental input is set equal to -7dBm per tone. The result indicates that the IMD component can be varied between -62dBm and -33dBm , as the baseband signal is tuned from 1mV to 90mV . The biasing voltage of the diode predistorter is approximately 0.3V .

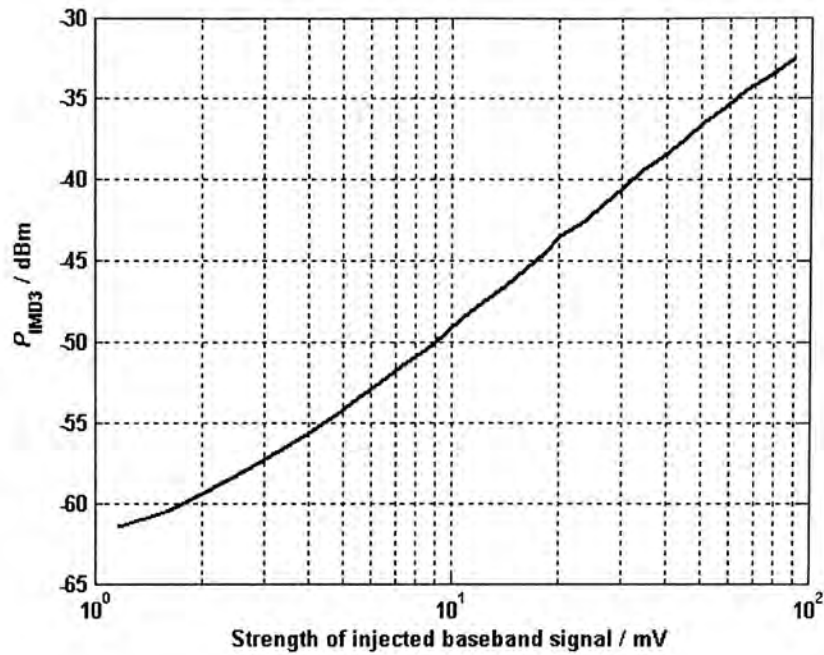


Fig. 6.4 IMD performance under baseband signal injection

6.1.2 Small Signal Amplifier

Fig. 6.5 and Fig. 6.6 show the schematic diagram and the physical view of the small signal amplifier. The active device used is MESFET CFY30 from Infineon Technologies. Gate and drain bias are established by using quarter-wavelength microstrips and radial stubs. The output matching network is optimized for maximum output power while the input matching network is optimized for higher gain. Additional by-pass capacitors are inserted into the drain circuitry to ensure stability at out-of-band frequencies.

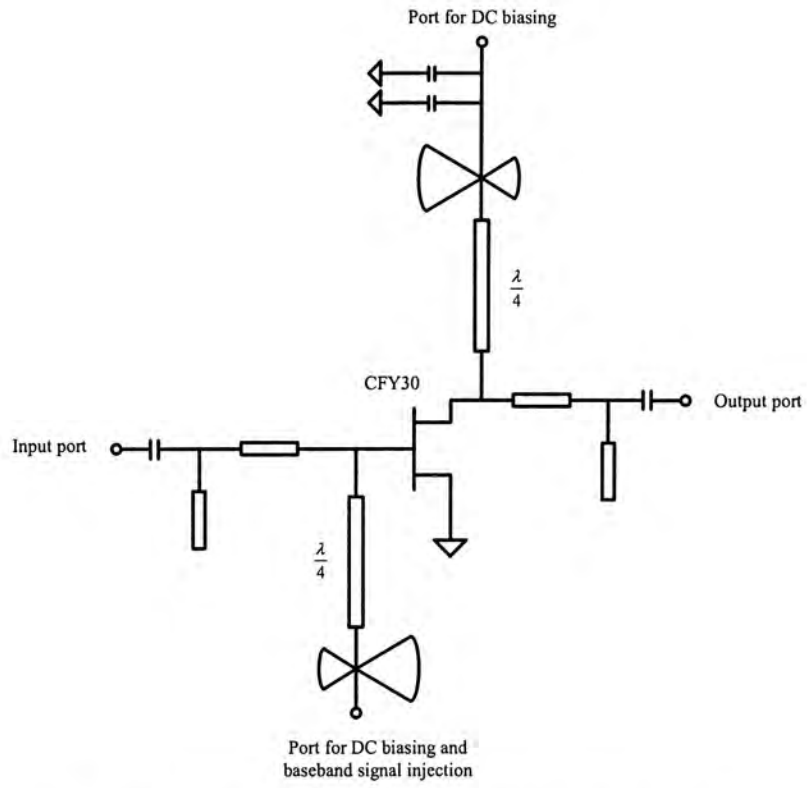


Fig. 6.5 Schematic of the small signal amplifier

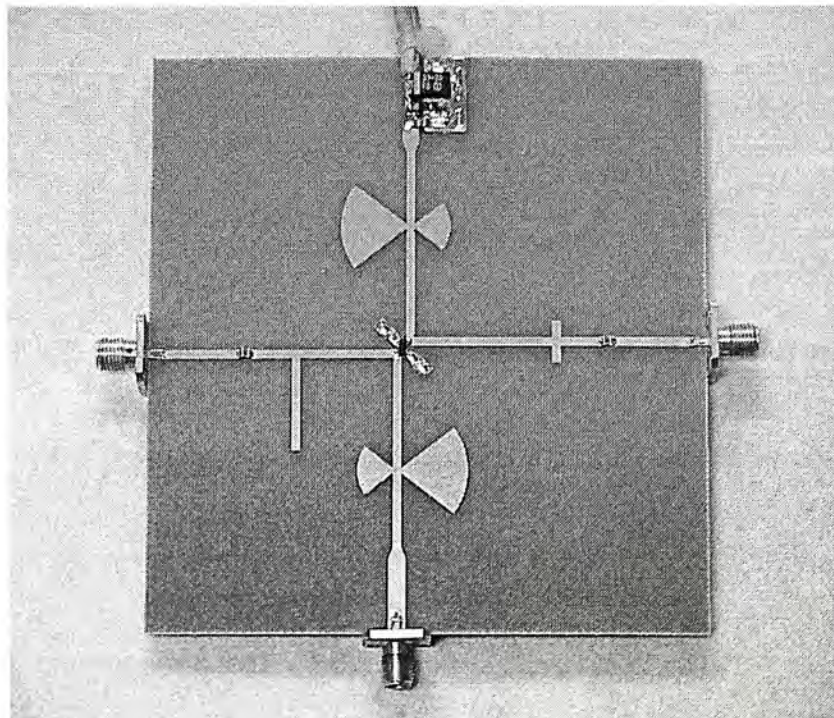


Fig. 6.6 Small signal amplifier constructed

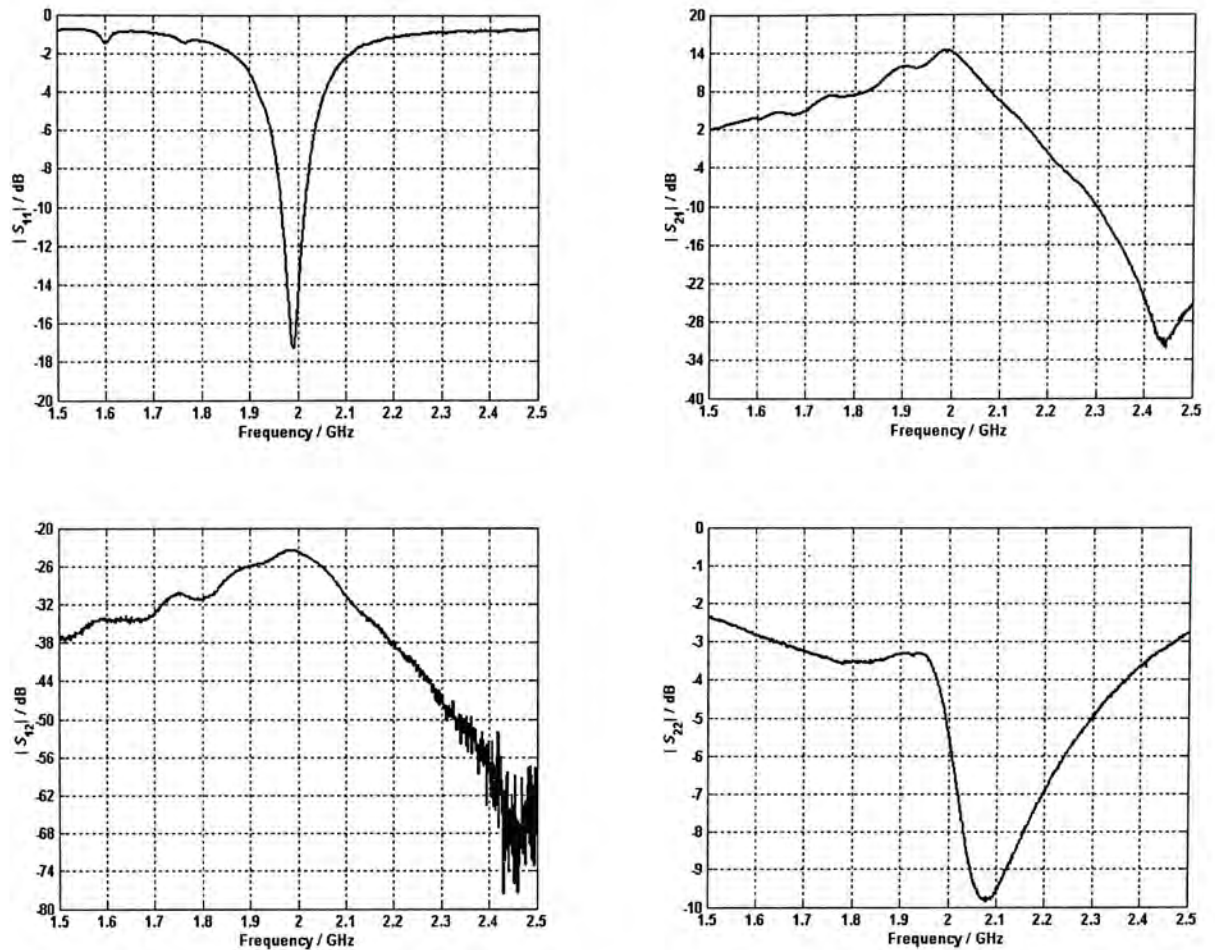


Fig. 6.7 S -parameter of the small signal amplifier

Fig. 6.7 shows the measured S -parameter of the constructed amplifier. The measured power gain, input return loss and output return loss of the amplifier is about 14dB, 10dB and 5dB, respectively. Fig. 6.8 depicts the power performance of the amplifier as the input power is swept from -10dBm to 6dBm. The output power is monitored using a spectrum analyzer with HPVVEE connection for automating the measurement. The output power of the amplifier measured at 1dB compression point is roughly 16dBm.

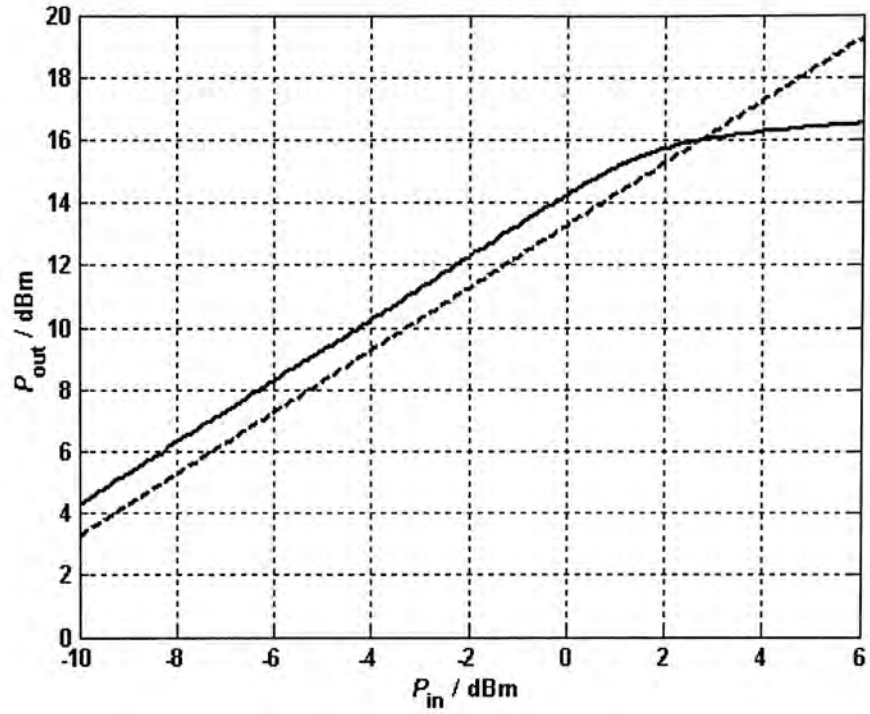
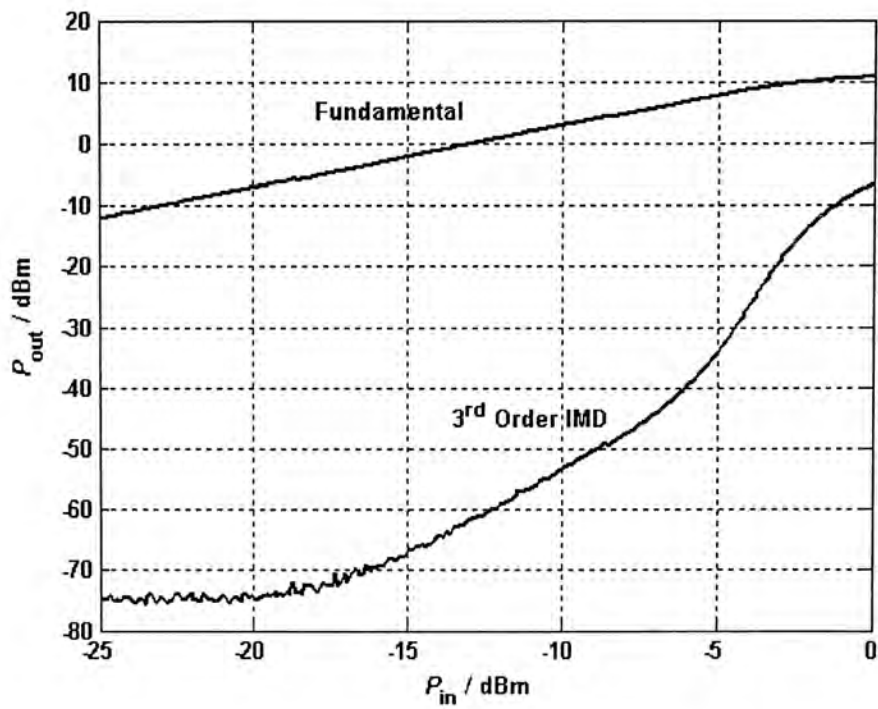
Fig. 6.8 $P_{1\text{dB}}$ of the small signal amplifier

Fig. 6.9 IMD performance of the small signal amplifier

Fig. 6.9 gives the measured IMD performance of the amplifier. Note that for low input power, less than -6dBm per tone, the IMD curve has a 3:1 slope. It implies

that the IMD signal generation is dominated by the third-order nonlinear function and the contribution from the high-order mixing terms is negligibly small (weakly nonlinear response).

6.1.3 Medium Power Amplifier

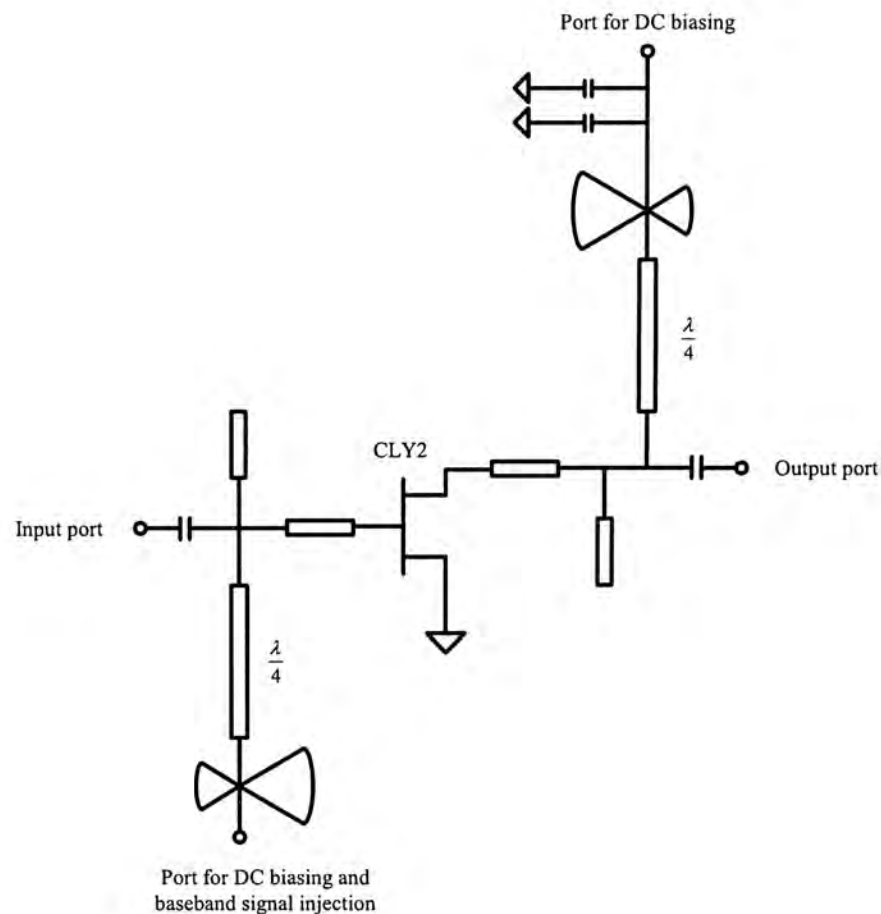


Fig. 6.10 Schematic of the medium power amplifier

Fig. 6.10 shows the circuit diagram of the medium power amplifier. The active device employed is MESFET CLY2 from Infineon Technologies. Input matching network is optimized for gain while the output matching network is optimized for maximum output power. The physical appearance of the power amplifier is given in Fig. 6.11.

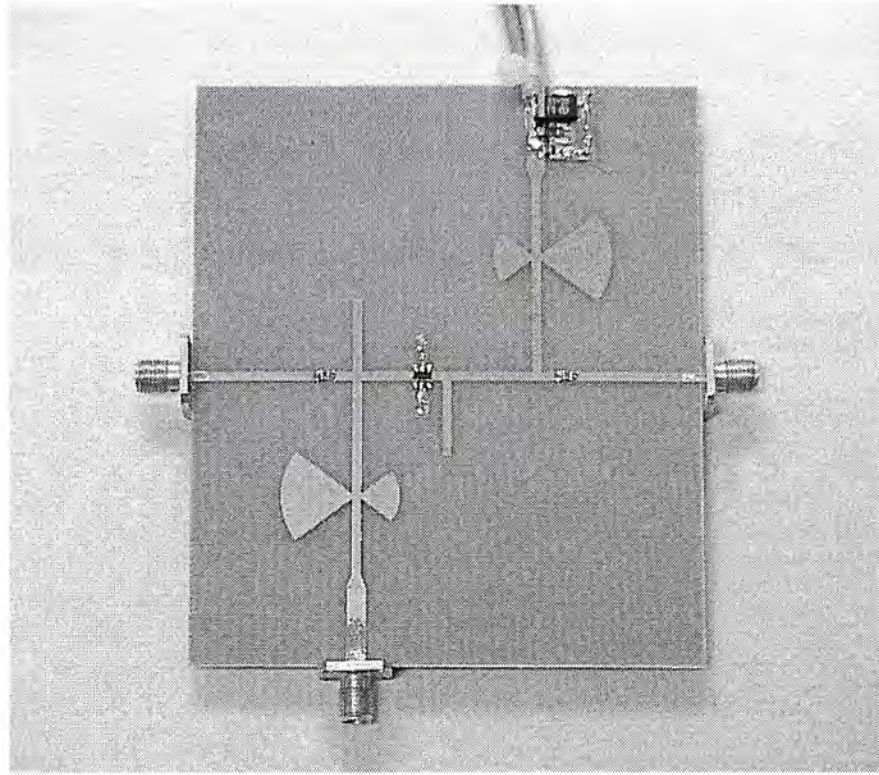
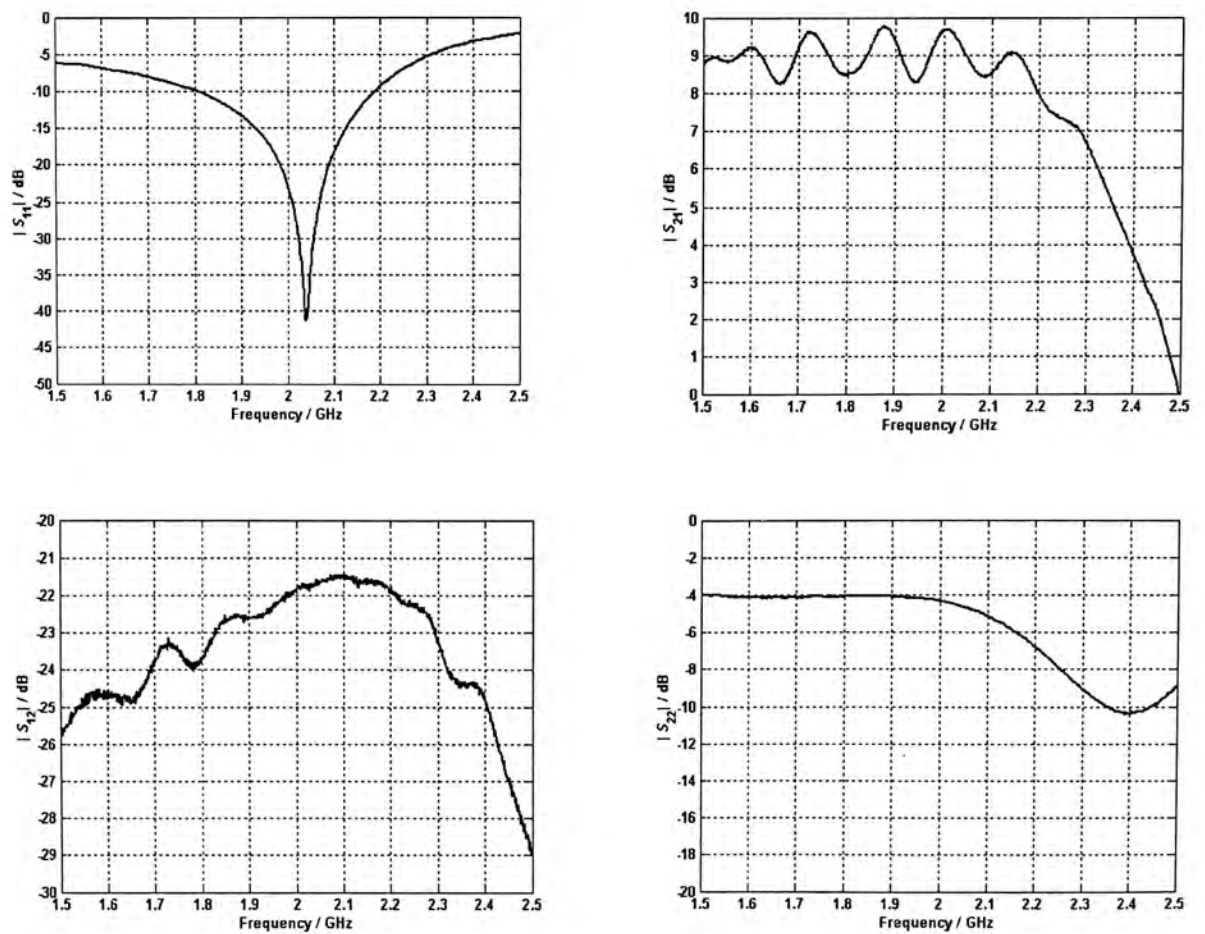


Fig. 6.11 Medium power amplifier constructed

Fig. 6.12 S -parameter of the medium power amplifier

According to Fig. 6.12, the measured gain, input return loss and output loss is 9dB, 20dB and 4dB respectively. The power amplifier has an output power of approximately 23.5dBm at 1dB compression point (Fig. 6.13). The measured IMD performance of the amplifier is shown in Fig. 6.14.

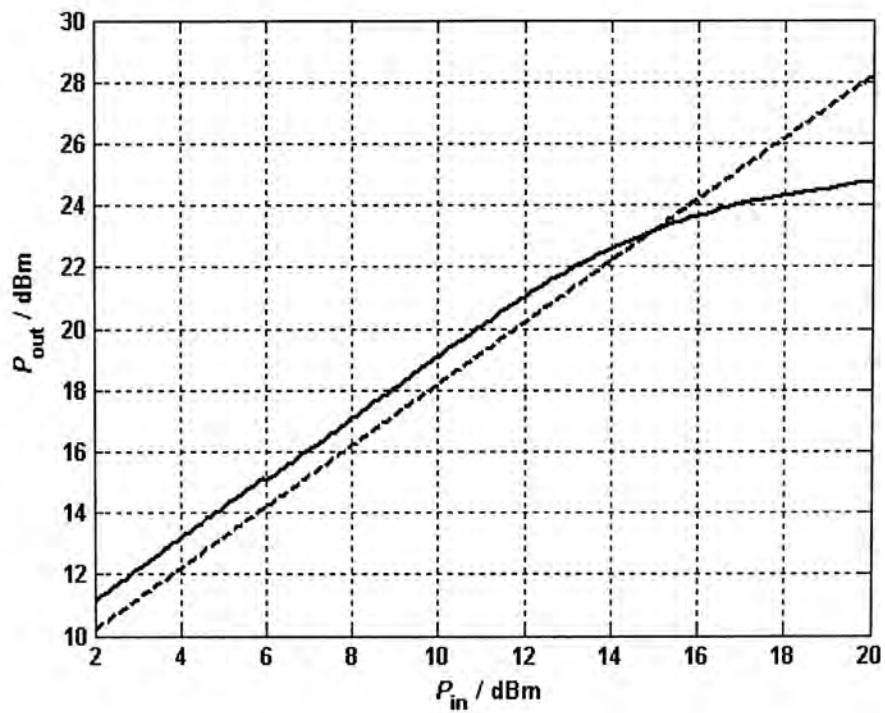


Fig. 6.13 P_{1dB} of the medium power amplifier

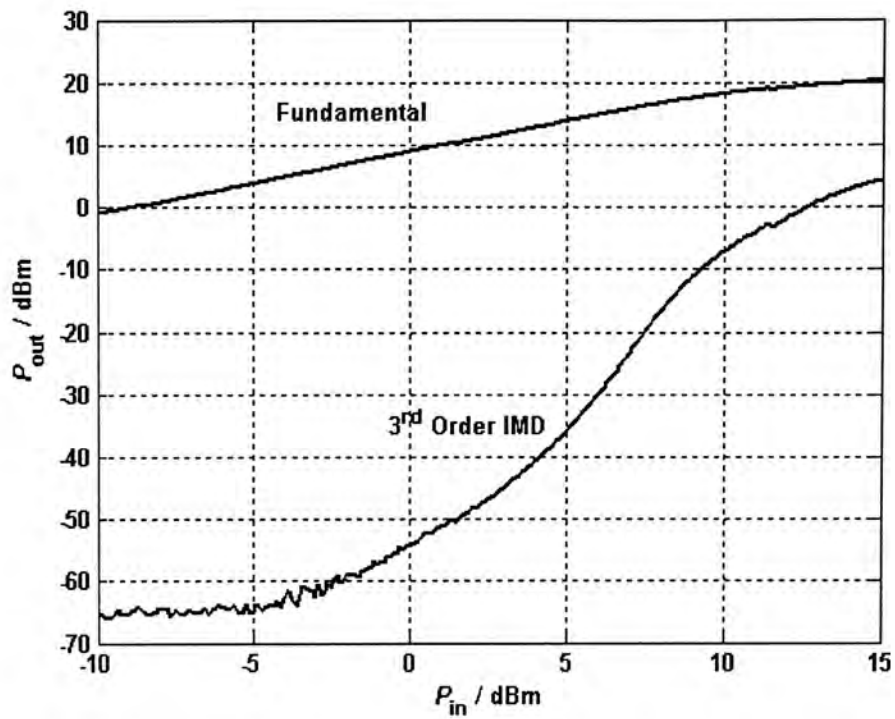


Fig. 6.14 IMD performance of the medium power amplifier

6.1.4 Baseband Signal Generation Circuit

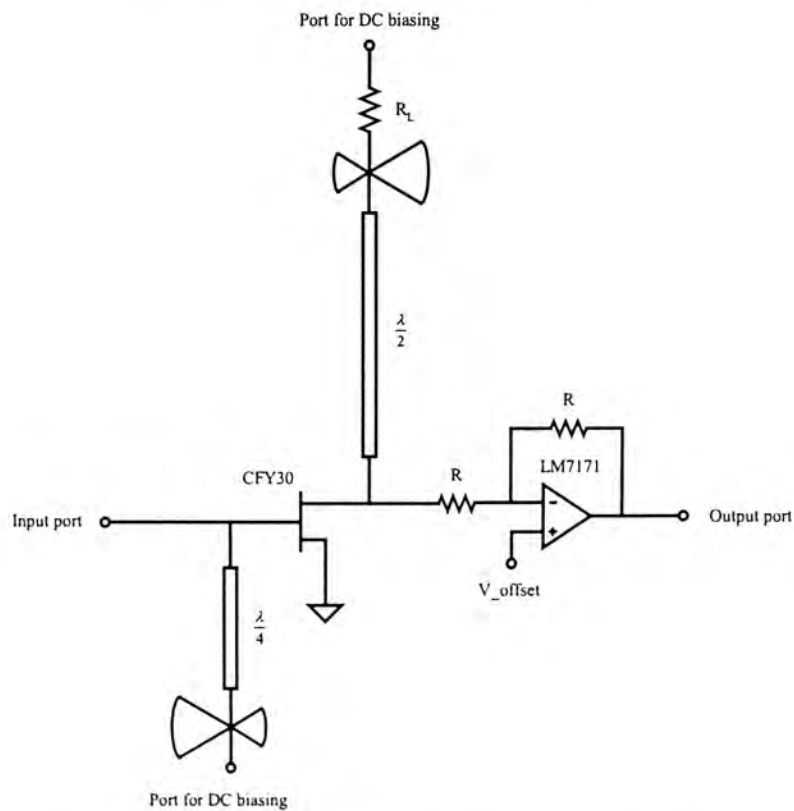


Fig. 6.15 Schematic of the generation circuit

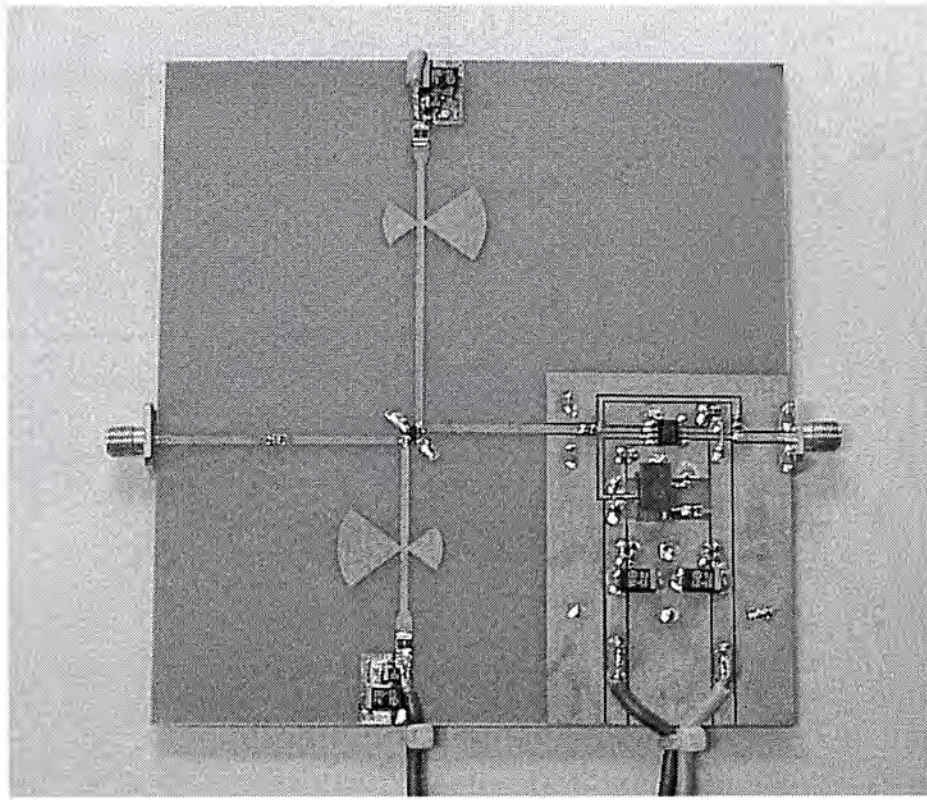


Fig. 6.16 Baseband signal generation circuit constructed

Fig. 6.15 and Fig. 6.16 show the schematic diagram of the generation circuit and the constructed hardware, respectively. For effective generation of the baseband signal, a MESFET CFY30 from Infineon Technologies operating near pinch off is adopted. At the drain output, the fundamental and second-harmonic are suppressed by microstrip filters constructed. The extracted baseband signal is buffered by simple inverting amplifier (LM7171). DC voltage appearing at the input of the baseband amplifier is removed by applying an offset voltage to the non-inverting input of the op-amp. The use of DC blocking capacitor is avoided here to eliminate any phase shift that might be introduced to the extracted signal.

6.1.5 Baseband Amplifiers

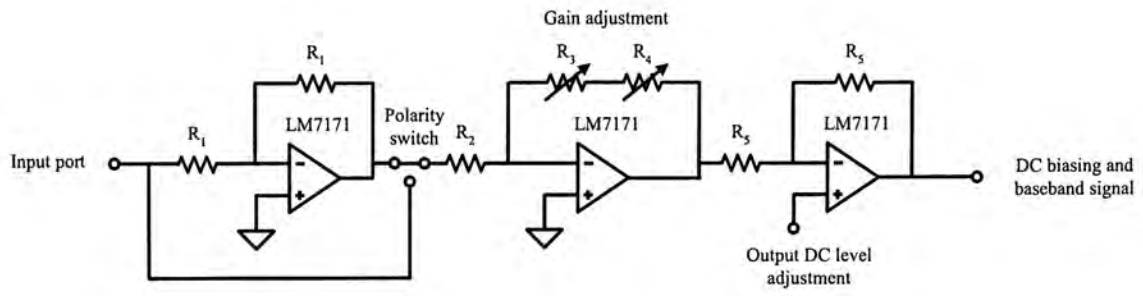


Fig. 6.17 Schematic of the baseband amplifiers

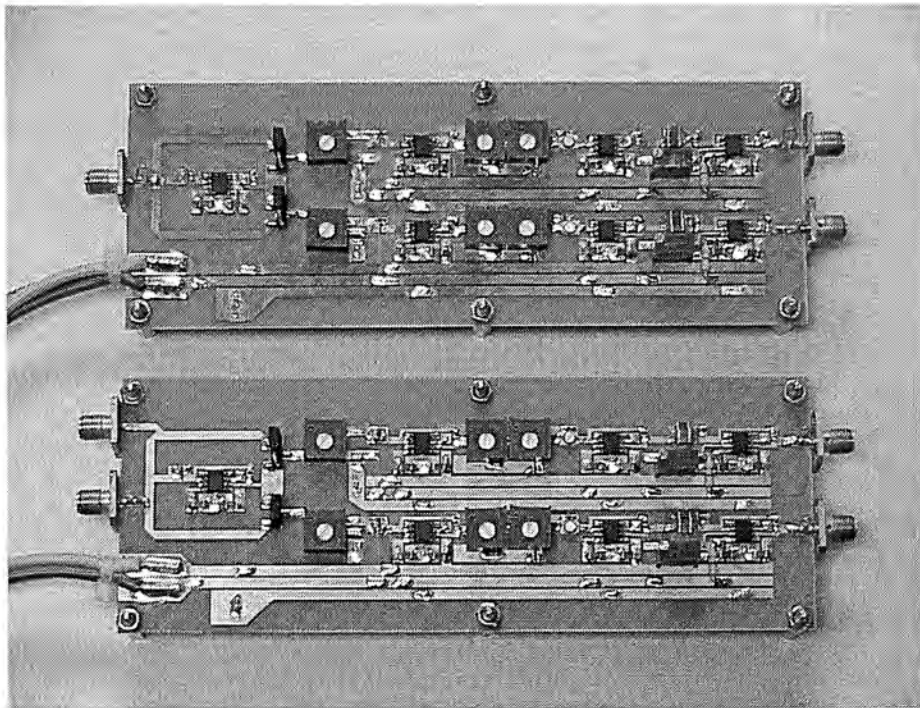


Fig. 6.18 Baseband amplifiers constructed

Amplification of baseband signal is achieved by the circuitry as shown in Fig. 6.17. The op-amps used are LM7171 from National Semiconductor. The phase angle (0° or 180°) is selected by polarity switch. Gain control is accomplished by the two variable resistors, R_3 and R_4 . The ratio of the two resistances is 10:1, so as to provide both coarse and fine adjustment. The DC level of the final output is tunable to provide proper biasing for RF amplifiers blocks. Fig. 6.18 shows the physical view

of the baseband amplifiers modules constructed.

6.2 Linearization of Amplifier with Predistortion Circuitry

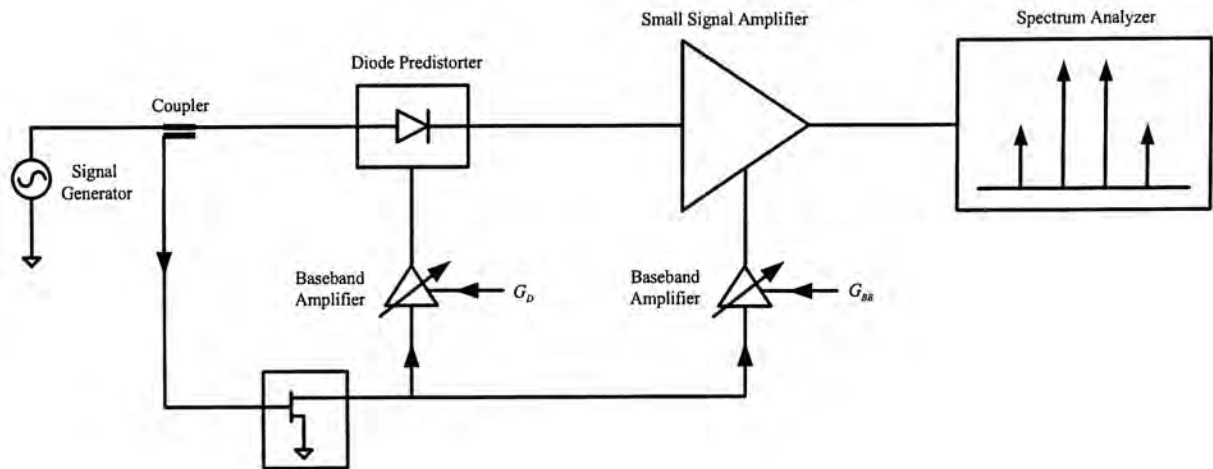
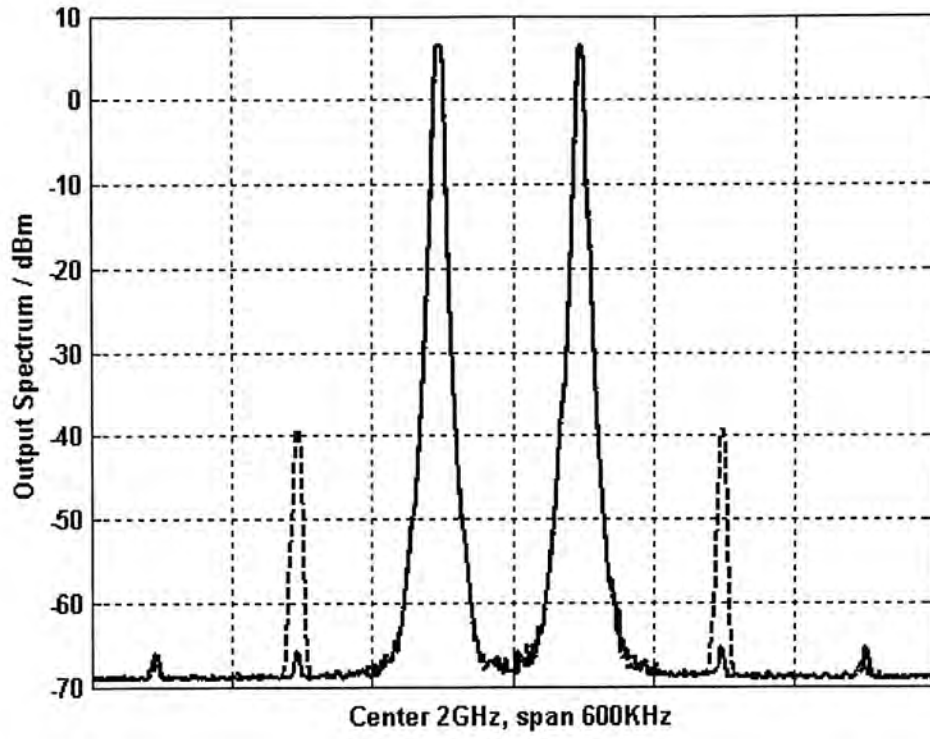


Fig. 6.19 Experimental setup

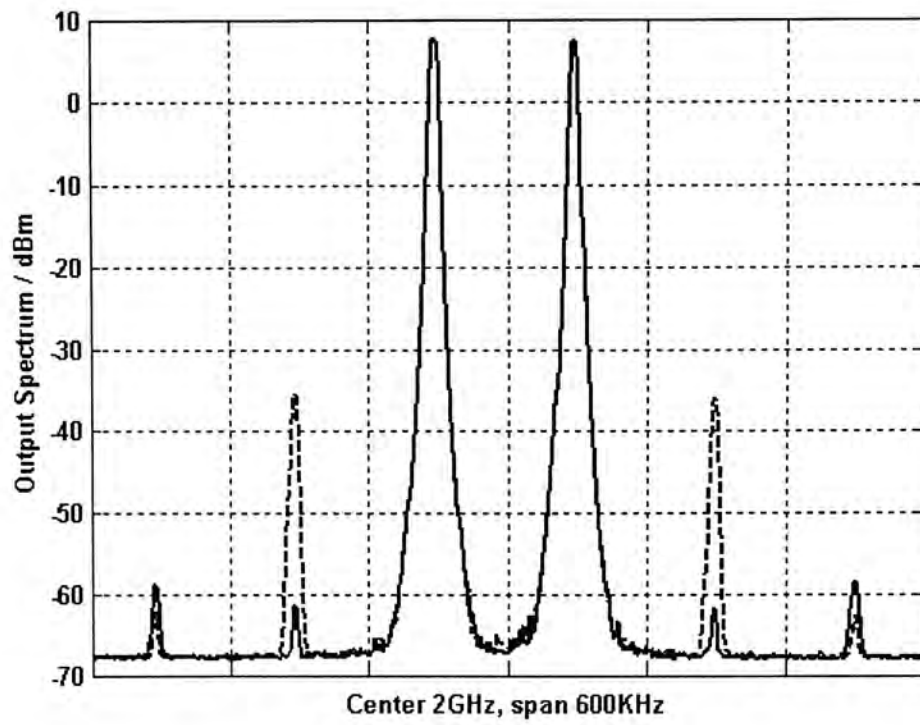
Fig. 6.19 shows the experimental setup for carrying out the measurement. The output spectrum of the system is monitored by a spectrum analyzer. HPVVEE [51] is employed for data acquisition and measurement automation.

6.2.1 Two-Tone Test

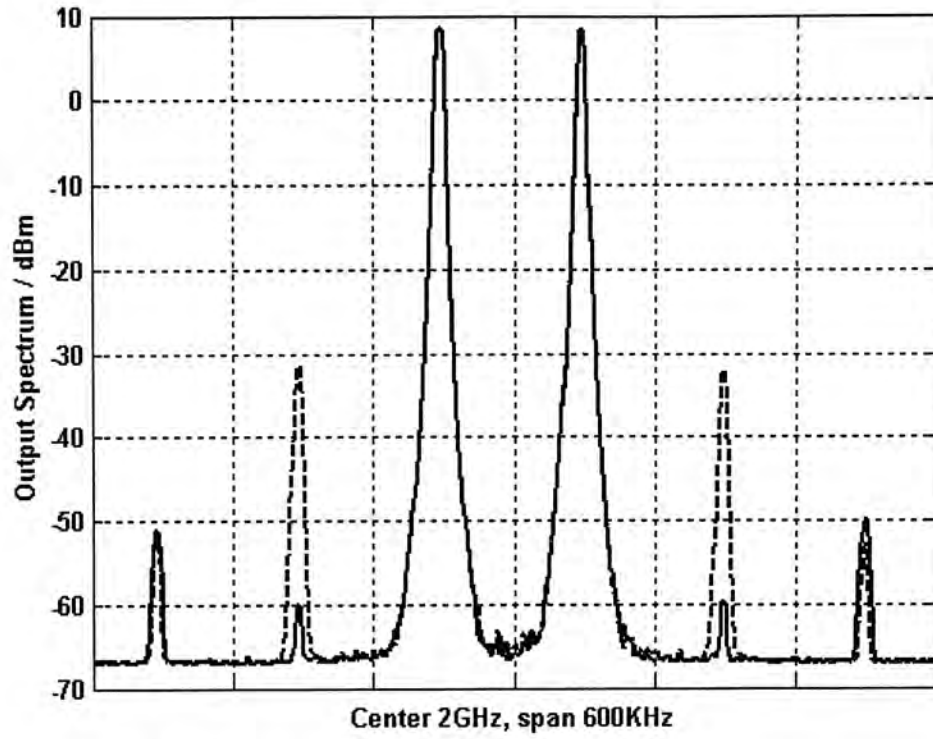
The DC bias of the diode predistorter is carefully adjusted to avoid the generation of high-order mixing products. The measured spectra of the output at three different output power levels (6.5dBm, 7.5dBm and 8.5dBm), with and without linearization are plotted in Fig. 6.20.



(a) Output power = 6.5dBm per tone



(b) Output power = 7.5dBm per tone



(c) Output power = 8.5dBm per tone

Fig. 6.20 Measured spectra of two-tone test

Output power (dBm)	IMD without linearization (dBm)	IMD with linearization (dBm)	Factor of improvement (dB)
6.5	-39.2	-65.8	26.6
7.5	-35.6	-61.4	25.8
8.5	-31.4	-60.0	28.6

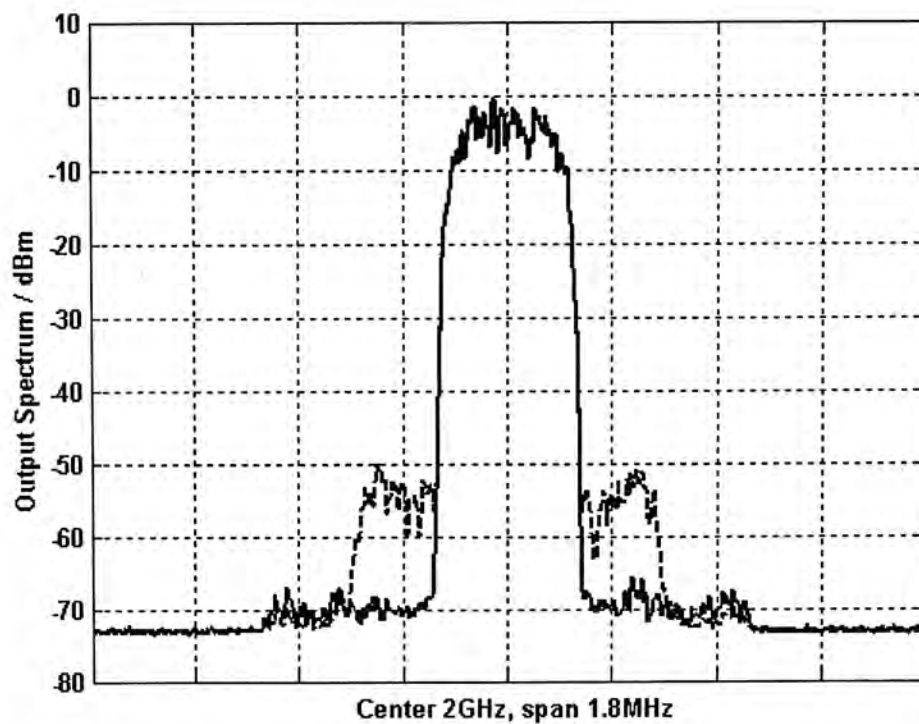
Table 6.2 Summary of two-tone test results

The measured IMD performances of the two-tone tests are summarized in Table 6.2. It can be observed that, by adjusting the strength of the baseband signal injected into the diode predistorter and the RF amplifier, a substantial amount of IMD suppression (>25dB) is achieved. For the purpose of comparison, conventional

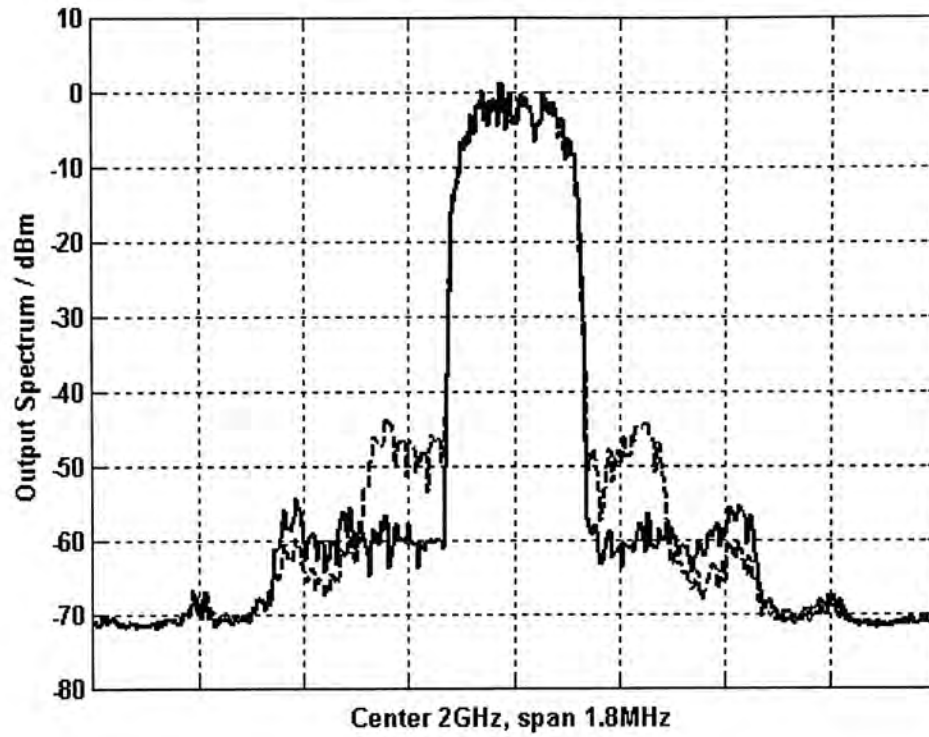
baseband approach is also implemented. This is done by removing the diode predistorter and injecting baseband signal into the amplifier only. In this case, it is observed that the IMD level is suppressed by less than 1dB at all the three power levels.

6.2.2 Vector Signal Test

Fig. 6.21 shows the output spectra of the system in response to a PHS input signal, at average output power levels of 14dBm and 15dBm.



(a) Average output power of 14dBm



(a) Average output power of 15dBm

Fig. 6.21 PHS signal test results

At average output power of 14dBm, a reduction in Adjacent Channel Power Ratio (ACPR) of almost 15dB is observed. In the second case (15dBm), the first side-lobes are suppressed by about 12dB. The increased side-lobes power level is mainly due to the contribution from the higher-order mixing products when operate closer to saturation.

6.2.3 Dynamic Range Evaluation

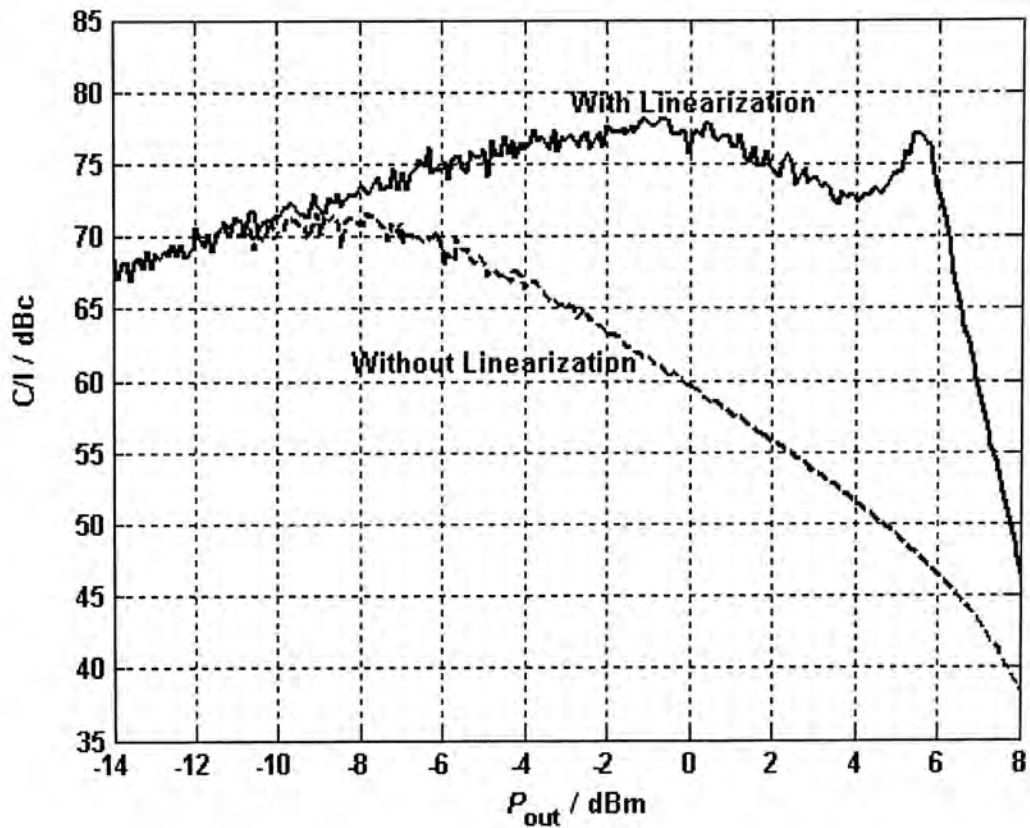


Fig. 6.22 Measured C/I ratio versus output power level

Fig. 6.22 shows the measured carrier-to-intermodulation ratio (C/I) as the output power is varied. The 1dB compression point of the system is 16dBm. The system is optimized for minimum third-order IMD at an output power level of 6dBm per tone. It can be seen from the diagram that a C/I ratio of better than 70dBc is obtained over a wide range of output power level. At very low output power level, the result is limited only by linearity and noise performance of the measuring equipments. The degradation in C/I ratio when the system is operated beyond the optimized point can be explained by the higher-order mixing effects.

6.3 Linearization of Multi-Stage Amplifying System

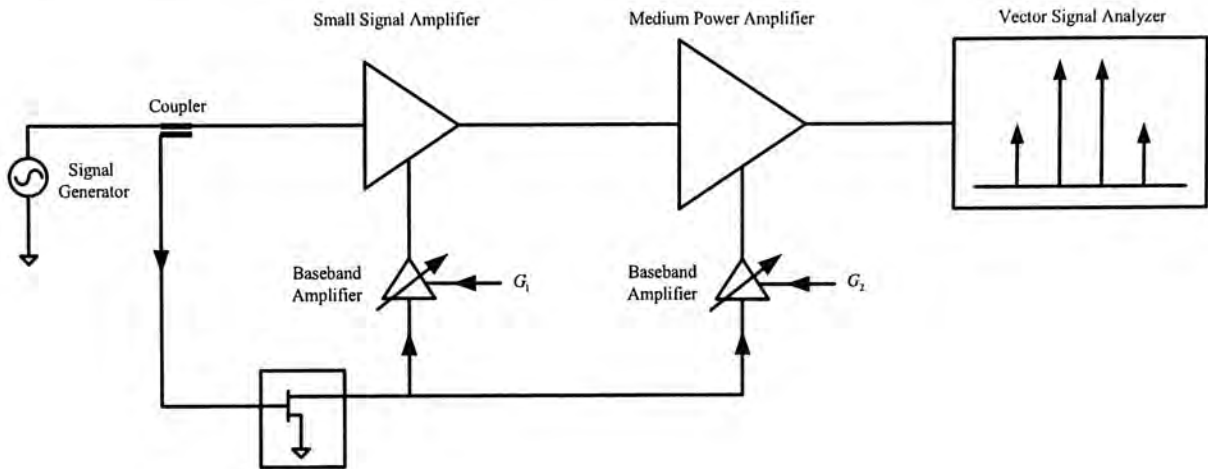


Fig. 6.23 Experimental setup

Fig. 6.23 shows the experimental setup which consists of a driver amplifier, a main amplifier and the linearization circuits. The output signal is monitored by the vector signal analyzer HP89441A which is also capable of determining both the phase and magnitude of the measured signal. HPVVEE is adopted here for data manipulation and measurement automation.

6.3.1 Determination of Transfer and Gain Coefficients

With reference to the formulation in Chapter 5, the expression for the IMD output of a two-stage amplifying system is:

$$|d_2| = \left| A e^{j\kappa} + G_1 b_1 |T_1| e^{j\varphi_1} + G_2 b_2 |T_2| e^{j\varphi_2} \right| \quad (6.1)$$

The optimum gain coefficients may be derived as:

$$G_1 = \frac{-A}{b_1 |T_1|} \cdot \frac{\sin(\kappa - \varphi_2)}{\sin(\varphi_1 - \varphi_2)} \quad (6.2)$$

$$G_2 = \frac{A}{b_2|T_2|} \cdot \frac{\sin(\kappa - \varphi_1)}{\sin(\varphi_1 - \varphi_2)} \quad (6.3)$$

It is clear from the above expressions that the gain coefficients can readily be calculated if all the transfer coefficients (A , $b_1|T_1|$, $b_2|T_2|$, κ , φ_1 and φ_2) are known. The magnitudes of the transfer coefficients (A , $b_1|T_1|$, $b_2|T_2|$) can easily be found by power measurement while the phase angles (κ , φ_1 and φ_2) may be determined either by adopting the method introduced in [52] or by using a vector signal analyzer [53, 54]. In this experiment, the transfer coefficients are measured by the latter approach in conjunction with the steps and equations outlined in Table 6.3. Note that the gain coefficients (G_B and G_C) are chosen in such way that the third-order IMD signal is dominating and the higher-order mixing products are negligibly small. Subsequently, the extracted values of the system parameters are tabulated in Table 6.4 for reference. Table 6.5 shows the calculated optimum gain coefficients and IMD performance for the various injection methods.

G_1	G_2	d_2 (By measurement)	Formulas for parameter extraction
0	0	d_A	$Ae^{j\kappa} = d_A$
G_B	0	d_B	$b_1 T_1 e^{j\varphi_1} = \frac{d_B - d_A}{G_B}$
0	G_C	d_C	$b_2 T_2 e^{j\varphi_2} = \frac{d_C - d_A}{G_C}$

Table 6.3 Procedures for the determination of transfer coefficients

A	κ	$b_1 T_1 $	φ_1	$b_2 T_2 $	φ_2
14.04	168.2°	3.33	293.6°	1.76	326.5°

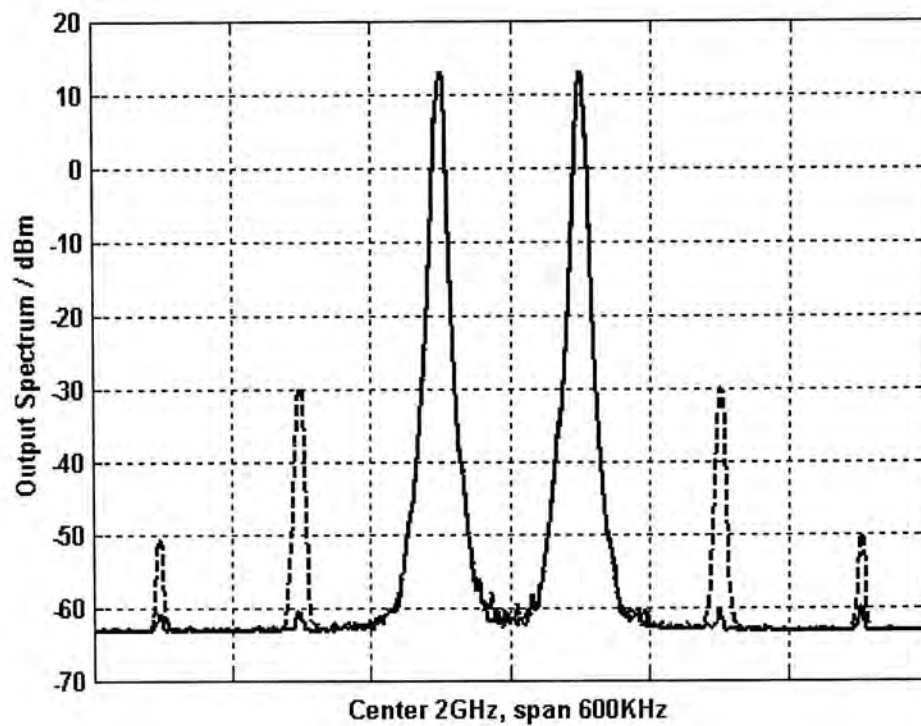
Table 6.4 Extracted parameters of the experimental system

Point of Injection	Optimum G_1	Optimum G_2	Factor of improvement (dB)
Small signal amplifier	2.44	0	1.77
Medium power amplifier	0	7.41	8.65
Both	-2.87	11.96	∞

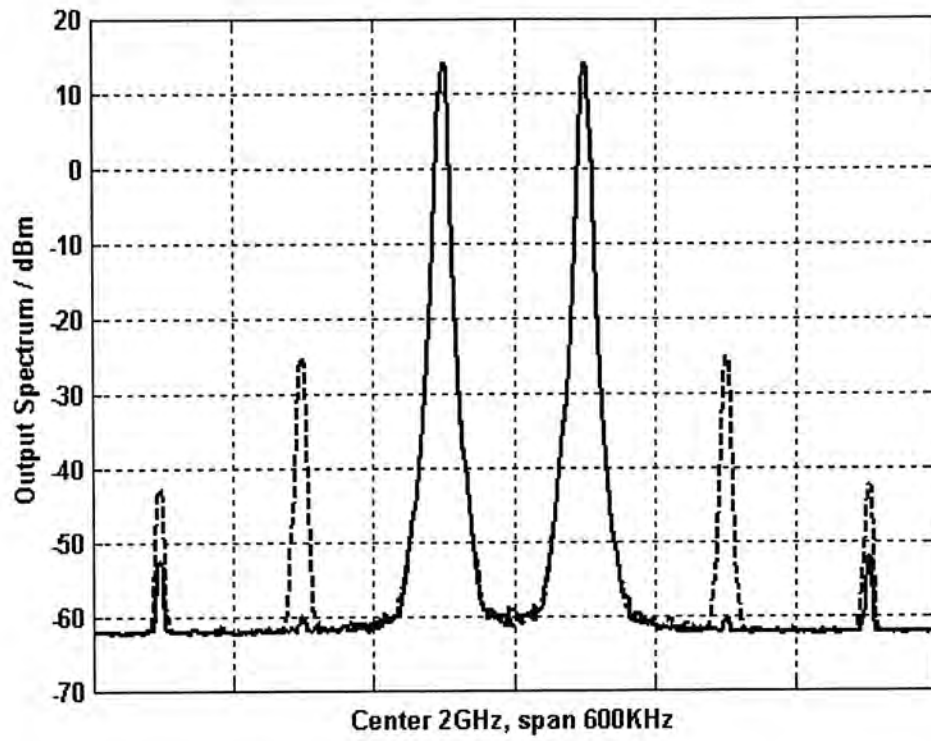
Table 6.5 Predicted performance of the experimental system

6.3.2 Two-Tone Test

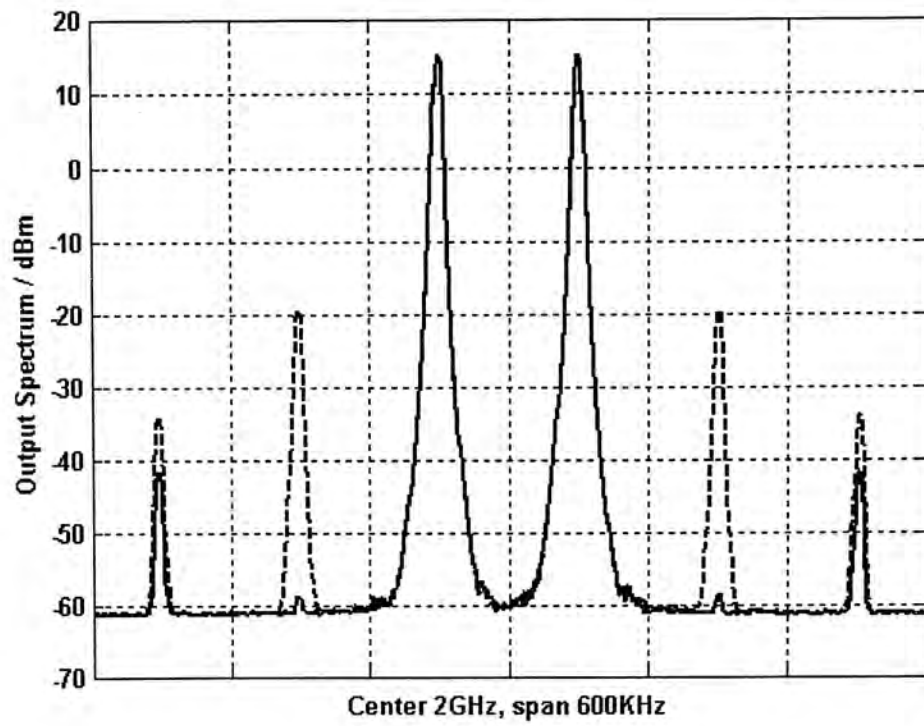
The measured output spectra of the system, with and without linearization, at various power levels (13dBm, 14dBm and 15dBm) are plotted in Fig. 6.24. The measured IMD performances of the system under various operating conditions are tabulated in Table 6.6. Note that the IMD level is suppressed by more than 30dB by using the generalized baseband signal injection method (dual injections).



(a) Output power of 13dBm per tone



(b) Output power of 14dBm per tone



(c) Output power of 15dBm per tone

Fig. 6.24 Two-tone test results

Output power (dBm)	IMD without linearization (dBm)	IMD with linearization (dBm)	Factor of improvement (dB)
13	-29.8	-60.7	30.9
14	-24.3	-57.2	32.9
15	-19.4	-59.0	39.6

Table 6.6 Summary of two-tone test results

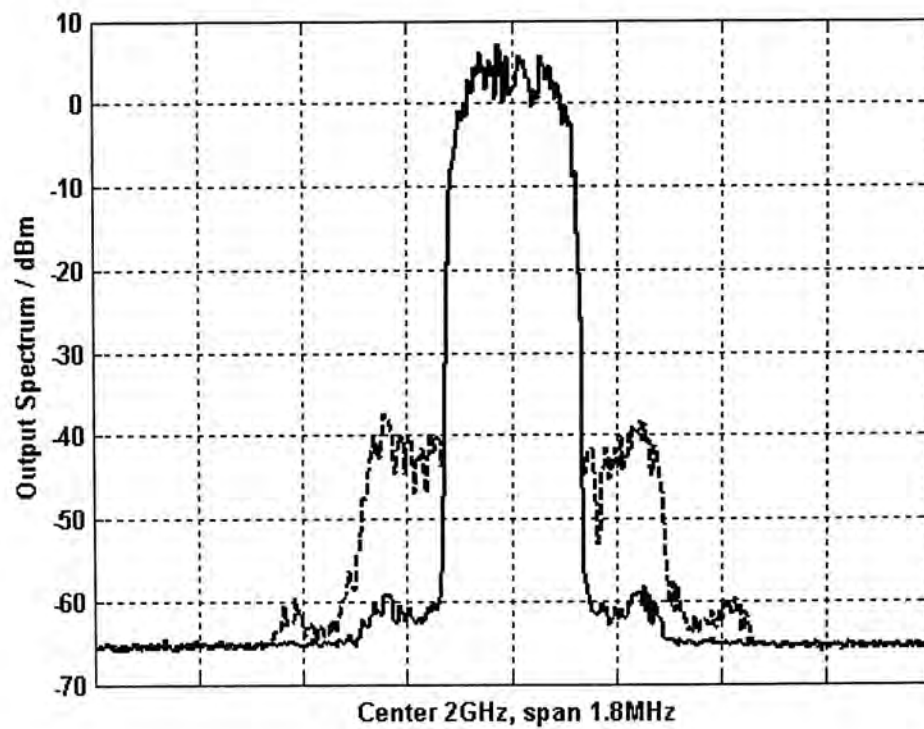
For verification purposes, the operating parameters of the system at an output power of 14dBm with various injection conditions are measured and tabulated in Table 6.7. Comparing these results with those calculated values shown in Table 6.5, excellent agreements are observed in all cases.

Point of Injection	Optimum G_1	Optimum G_2	Factor of improvement (dB)
Small signal amplifier	2.27	0	1.6
Medium power amplifier	0	6.72	8.2
Both	-2.99	12.60	32.9

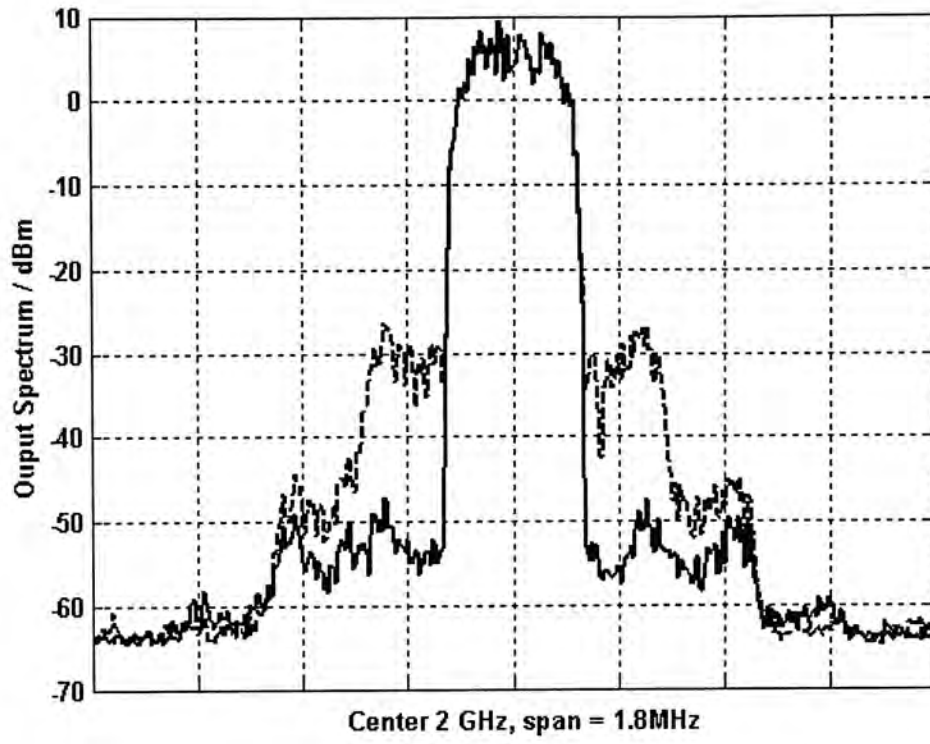
Table 6.7 Measured performance of the experimental system

6.3.3 Vector Signal Test

Fig. 6.25 shows the output spectra (PHS input signal) at average output power of 21 and 23dBm. It is found that the value of ACPR is improved by almost 20dB. Again, higher side-lobes level is observed at increased output power (23dBm) which is mainly contributed by the fifth-order mixing products near saturation



(a) Average output power of 21dBm



(b) Average output power of 23dBm

Fig. 6.25 PHS signal test results

6.3.4 Dynamic Range Evaluation

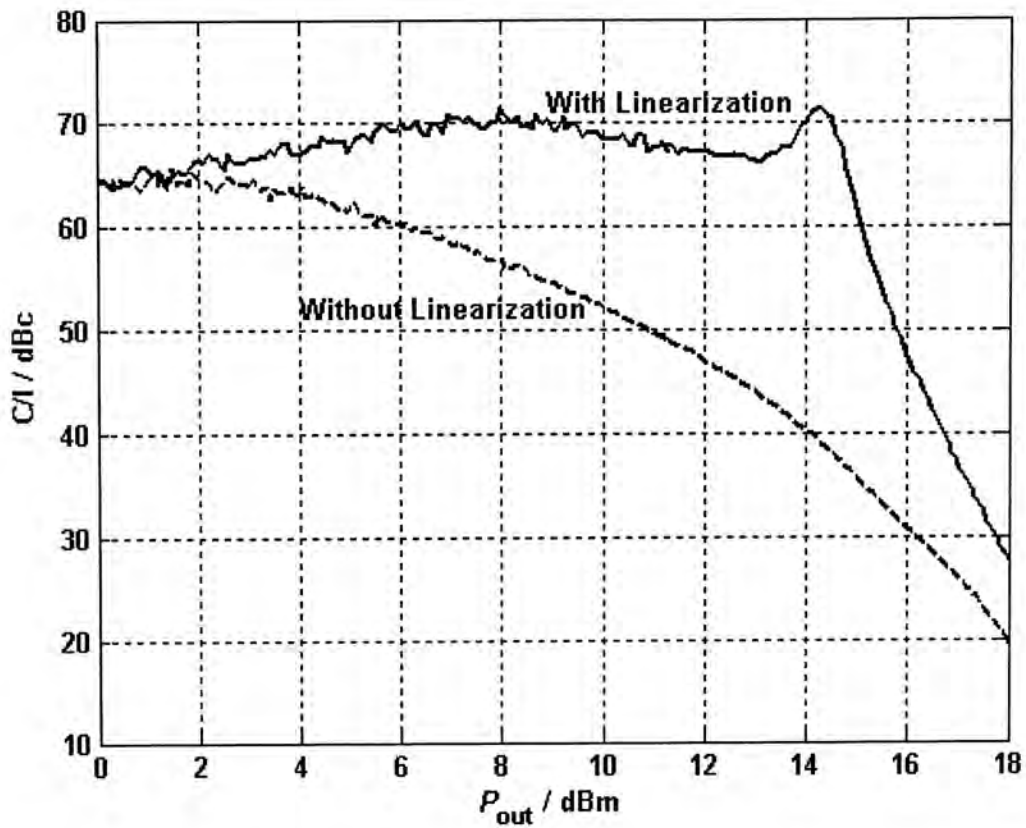


Fig. 6.26 Measured C/I ratio versus output power

Fig. 6.26 shows the plot of carrier-to-IMD ratio (C/I) versus output power of the system, with and without linearization. The 1dB compression point of the system is 23.5dBm. The IMD performance is optimized at an output power of 14dBm. A C/I ratio better than 65dBc is observed with the proposed method over a wide output power range. At low output power level, the result is limited only by linearity and noise performance of the measuring equipment. Note that the C/I ratio degrades as the output power increases towards the 1dB compression point as expected.

Chapter 7 Conclusion and Future Work

Linearization techniques play a crucial role in contemporary and future wireless communication systems. In order to support new high data-rate applications in the increasingly crowded spectrum, spectral efficient modulation schemes have to be adopted. Amplification of these signals places stringent linearity requirement on transmitter design, especially the RF power amplifier. Linearization technique is a mean to satisfy both low distortion requirement and high power efficiency requirements of amplifiers.

In this thesis, a novel linearization approach based on the generalized baseband signal injection concept has been presented. A mathematical foundation of the proposed method has been formulated using the Volterra series theory. From the derived expressions, the operating conditions for optimal suppression of IMD are deduced. Applications of the generalized baseband signal injection method to the linearization of various amplifying configuration have been presented. For demonstration, experimental systems have been setup and extensive performance evaluation using two-tone and vector signal has been conducted. The measured results have confirmed the validity of the proposed method. Moreover, substantial IMD improvement has been observed over a wide range of output power level. A

simple method to calculate the gain coefficients from the measured output signals of the system has also developed.

For future work, the generalized baseband signal injection method may be extended to the suppression of fifth- and higher-order IMD components. Also, the bandwidth limitation of the proposed method should be addressed. Moreover, miniaturization of the linearization circuitry using state-of-the-art integration process such as LTCC and RFIC technologies are recommended.

References

- [1] P. B. Kenington, *High-Linearity RF Amplifier Design*, Norwood, MA, Artech House, 2000.
- [2] M. R. Moazzam, and C. S. Aitchison, "A low third order intermodulation amplifier with harmonic feedback circuitry," *IEEE MTT-S Int. Microwave Symp. Dig.*, vol. 2, pp. 827-830, 1996.
- [3] D. Jing, W. S. Chan, S. M. Li, C. W. Li, "New linearization method using interstage second harmonic enhancement", *IEEE Microwave and Guided Wave Lett.*, vol. 8, no. 11, pp. 402-404, Nov. 1998.
- [4] Y. Hu, J. C. Mollier, and J. Obregon, "A new method of third-order intermodulation reduction in nonlinear microwave systems," *IEEE Trans. Microwave Theory and Tech.*, vol. 34, no. 2, pp. 245-250, Feb. 1986.
- [5] Y. Yang, and B. Kim, "A new linear amplifier using low-frequency second-order intermodulation component feedforwarding", *IEEE Microwave and Guided Wave Lett.*, vol. 9, no. 10, pp. 419-421, Oct. 1999.
- [6] C. W. Fan, K. K. M. Cheng, "Amplifier linearization using simultaneous harmonic and baseband injection", *IEEE Microwave and Wireless Components Lett.*, vol. 11, no. 10, pp. 404-406, Oct. 2001.

- [7] N. Potheary, *Feedforward Linear Power Amplifier*, Norwood, MA, Artech House, 1999.
- [8] K. J. Parsons, P. B. Kenington, "The efficiency of a feedforward amplifier with delay loss", *IEEE Trans. on Veh. Technol.*, vol. 43, no. 2, pp. 407-412, May. 1994.
- [9] P. B. Kenington, "Efficiency of feedforward amplifiers", *IEE Proc. on Circuits, Devices and Systems*, vol. 139, no. 5, pp. 591-593, Oct. 1992.
- [10] J. K. Cavers, "Adaptation behavior of a feedforward amplifier linearizer", *IEEE Trans. on Veh. Technol.*, vol. 44, no.1, pp. 31-40, Feb. 1995.
- [11] S. J. Grant, J. K. Cavers, P. A. Goud, "A DSP controlled adaptive feedforward amplifier linearizer", *IEEE International Conference on Universal Personal Communications*, vol.2, pp. 788-792, 1996.
- [12] S. Narahashi, T. Nojima, "Extremely low-distortion multi-carrier amplifier-self-adjusting feed-forward (SAFF) amplifier", *IEEE International Conference on Communications*, vol. 3 pp. 1485-1490, 1991.
- [13] G. Zhao, F. M. Ghannouchi, F. Beaugard, A. B. Kouki, "Digital implementations of adaptive feedforward amplifier linearization techniques", *IEEE MTT-S International Microwave Sympo. Dig.*, vol.2, pp. 543-546, 1996.
- [14] J. G. McRory, R. H. Johnston, "An RF amplifier for low intermodulation

- distortion”, *IEEE MTT-S Int. Microwave Sympo. Dig.*, vol. 3, pp. 1741-1744, 1994.
- [15] M. Bolorian, J. P. McGeehan, “The frequency-hopped Cartesian feedback linear transmitter”, *IEEE Trans. on Veh. Technol.*, vol. 45, no. 4, pp. 688-706, Nov. 1996.
- [16] M. Faulkner, “An automatic phase adjustment scheme for RF and cartesian feedback linearizers”, *IEEE Trans. on Veh. Technol.*, vol. 49, no. 3, pp. 956-964, May, 2000.
- [17] J. S. Cardinal, F. M. Ghannouchi, “A new adaptive double envelope feedback (ADEF) linearizer for solid state power amplifiers”, *IEEE Trans. Microwave Theory and Tech.*, vol. 43, no. 7, pp. 1508-1515, Jul. 1995.
- [18] C. S. Yu, W. S. Chan, W. L. Chan, “1.9 GHz low loss varactor diode pre-distorter”, *Electronics Lett.*, vol. 35, no. 20, Sept, 1999.
- [19] K. Yamauchi, K. Mori, M. Nakayama, Y. Mitsui, T. Takagi, “A microwave miniaturized linearizer using a parallel diode with a bias feed resistance”, *IEEE Trans. Microwave Theory and Tech.*, vol. 45, no. 12, pp. 2431-2435, Dec. 1997.
- [20] K. Yamauchi, K. Mori, M. Nakayama, Y. Itoh, Y. Mitsui, O. Ishida, “A novel series diode linearizer for mobile radio power amplifiers”, *IEEE MTT-S Int. Microwave Sympo. Dig.*, vol. 2, pp. 831-834, 1996.

- [21] R. C. Tupynamba, E. Camargo, "MESFET nonlinearities applied to predistortion linearizer design", *IEEE MTT-S Int. Microwave Sympo. Dig.*, vol. 2, pp. 955-958, 1992.
- [22] M. G. Kim, C. H. Kim, H. K. Yu, J. Lee, "An FET-level linearization method using a predistortion branch FET", *IEEE Microwave and Guided Wave Lett.*, vol. 9, no. 6, pp. 233-235, Jun. 1999.
- [23] J. Yi, Y. Yang, M. Park, W. Kang, B. Kim, "Analog predistortion linearizer for high-power RF amplifiers", *IEEE Trans. Microwave Theory and Tech.*, vol. 48, no. 12, pp. 2709-2713, Dec. 2000.
- [24] Y. Kim, Y. Yang, S. Kang, and B. Kim, "Linearization of 1.85 GHz amplifier using feedback predistortion loop," *IEEE MTT-S Int. Microwave Sympo. Dig.*, vol. 3, pp. 1675-1678, 1998.
- [25] M. Faulkner, "Amplifier linearization using RF feedback and feedforward techniques", *IEEE Trans. on Veh. Technol.*, vol. 47, no. 1, pp. 209-215, Feb. 1995.
- [26] H. M. Park, D. H Baek, K. I. Jeon, S. Hong, "A predistortion linearizer using envelope-feedback technique with simplified carrier cancellation scheme for class-A and class-AB power amplifiers", *IEEE Trans. Microwave Theory and Tech.*, vol. 48, no. 6, pp. 898-904, Jun. 2000.

- [27] F. H. Raab, "Intermodulation distortion in Kahn-technique transmitters", *IEEE Trans. Microwave Theory and Tech.*, vol. 44, no. 12, pp. 2273-2278, Dec. 1996.
- [28] F. H. Raab, B. E. Sigmon, R. G. Myers, R. M. Jackson, "L-band transmitter using Kahn EER technique", *IEEE Trans. Microwave Theory and Tech.*, vol. 46, no. 12, pp. 2220-2225, Dec. 1998.
- [29] D. C. Cox, "Linear amplification with nonlinear components", *IEEE Trans. Commun.*, vol. 28, pp. 1942-1945, Dec. 1974.
- [30] X. Zhang, P. Nanawa, L. E. Larson P. M. Asbeck, "A gain/phase imbalance minimization technique for LINC transmitter", *IEEE MTT-S Int. Microwave Sympo. Dig.*, vol. 2, pp. 801-804, 2001.
- [31] D. J. Jennings, J. P. McGeehan, "A high-efficiency RF transmitter using VCO-derived synthesis: CALLUM", *IEEE Trans. Microwave Theory and Tech.*, vol. 47, no. 6, pp. 715-721, Jun. 1999.
- [32] K. Y. Chan, A. Bateman, "Analytical and measured performance of the combined analogue locked loop universal modulator (CALLUM)", *IEE Proc. Commun.*, vol. 142, no. 5, pp. 297-306, Oct. 1995.
- [33] D. C. Cox, "Linear amplification by sampling techniques: a new application for delta coders", *IEEE Trans. Commun.*, vol. 23, no. 8, Aug. 1975.
- [34] M. Golio, *The RF and microwave handbook*, Boca Raton, Fla, CRC Press,

- 2001.
- [35] J. J. Bussgang, L. Ehrman, J. W. Graham. "Analysis of nonlinear systems with multiple input", *Proc. IEEE*, vol. 62, pp. 1088-1119, Aug. 1974.
- [36] S. A. Maas, D. Neilson, "Modeling MESFETs for intermodulation analysis of mixers and amplifiers", *IEEE Trans. Microwave Theory Tech.*, vol. 38, no. 12, pp. 1964-1971, Dec. 1990.
- [37] J. M. Golio, *Microwave MESFETs and HEMTs*, Boston, Artech House, 1991.
- [38] S. A. Maas, *Nonlinear Microwave Circuits*, Norwood, MA, Artech House, 1988.
- [39] Y. Hu, J. C. Mollier, and J. Obregon, "A new method of third-order intermodulation reduction in nonlinear microwave systems," *IEEE Trans. Microwave Theory and Tech.*, vol. 34, no. 2, pp. 245-250, Feb. 1986.
- [40] Y. Yang, and B. Kim, "A new linear amplifier using low-frequency second-order intermodulation component feedforwarding", *IEEE Microwave and Guided Wave Lett.*, vol. 9, no. 10, pp. 419-421, Oct. 1999.
- [41] A. M. Crossmun, S. A. Maas, "Minimization of intermodulation distortion in GaAs MESFET small-signal amplifiers", *IEEE Trans. Microwave Theory Tech.*, vol. 37, no. 9, pp. 1411-1417, Sept. 1989.
- [42] C. Y. Ho and D. Burgess, "Practical design of 2-4Ghz low intermodulation distortion GaAs FET amplifiers with flat gain response and low noise figure",

- Microwave J.*, vol. 34, pp. 295-300, 1991.
- [43] K. H. Ahn, Y. H. Jeong, S. H. Lee, "Effects of source and load impedance on the intermodulation products of GaAs FETs", *IEEE MTT-S International Microwave Sympo. Dig.*, vol. 1, pp. 469-472, 2000.
- [44] R. Nagy, J. Bartolic, B. Modlic, "GaAs MESFET small signal amplifier intermodulation distortion improvement by the second harmonic termination", *Mediterranean Electrotechnical Conf.*, vol. 1, pp. 358 -361, 1998.
- [45] J. Higgins, R. Kuvvas, "Analysis and improvement of intermodulation distortion in GaAs power FET's", *IEEE Trans. Microwave Theory Tech.*, vol. 28, no. 1, pp. 9-17, Jan. 1980.
- [46] J. C. Pedro, "Evaluation of MESFET nonlinear intermodulation distortion reduction by channel-doping control", *IEEE Trans. Microwave Theory Tech.*, vol. 45, no. 11, pp. 1989-1997, Nov. 1997.
- [47] J. K. Cavers, "Optimum table spacing in predistorting amplifier linearizers" *IEEE Trans. on Veh. Technol.*, vol. 48 no. 5, pp. 1699-1705 Sept. 1999.
- [48] X. Zhu, J. Zhou, W. Hong, H. Zhao, "A simple method to cut down configuration of feedforward power amplifier", *IEEE MTT-S Int. Microwave Symp. Dig.*, vol. 2, pp. 791-794, 2000.
- [49] A. Katz, A. Guida, R. Dorval, J. Dragone, "Input adaptive linearizer system",

-
- IEEE MTT-S Int. Microwave Symp. Dig.*, vol. 3, pp. 1499-1502, 2000.
- [50] Y. Wang, J. D. Fredrick, T. Itoh, "A novel DSP architecture of adaptive feedforward linearizer for RF amplifiers", *IEEE MTT-S Int. Microwave Symp. Dig.*, vol. 2, pp. 805-808, 2000.
- [51] Hewlett-Packard, user's guide for HP VEE 3.21.
- [52] Y. Yang, J. Yi, J. Nam, B. Kim, M. Park, "Measurement of two-tone transfer characteristics of high-power amplifiers", *IEEE Trans. Microwave Theory and Tech.*, vol. MTT-49, no 3, pp. 568-571, Mar. 2001.
- [53] Private conversation with Dr. C. W. Fan and Prof. K. K. M. Cheng.
- [54] Agilent Technologies 89441 A Getting Started Guide, <http://www.agilent.com>.

Author's Publications

1. C. S. Leung and K. K. M. Cheng, "A New Approach to Amplifier Linearization by the Generalized Baseband Signal Injection Method", to appear, *IEEE Microwave and Wireless Components Letters*, September, 2002.
2. C. S. Leung and K. K. M. Cheng, "A Novel Approach to Multi-Stage Amplifier Linearization by the Generalized Low-Frequency Signal Injection Method", submitted to *IEEE Transaction on Microwave Theory and Techniques*.

CUHK Libraries



003952987